2015

Nondestructive field assessment of flexible pavement and foundation layers

Jinhui Hu
Iowa State University

Nondestructive field assessment of flexible pavement and foundation layers

by

Jinhui Hu

A thesis submitted to the graduate faculty

in partial fulfillment of the requirements for the degree of

MASTER OF SCIENCE

Major: Civil Engineering (Geotechnical Engineering)

Program of Study Committee:
David J. White, Co-Major Professor
Pavana Vennapusa, Co-Major Professor
Igor Beresnev

Iowa State University

Ames, Iowa

2015

TABLE OF CONTENTS

LIST OF TABLES

LIST OF FIGURES

ABSTRACT

Falling weight deflectometer (FWD) and ground penetrating radar (GPR) are nondestructive test devices widely used by transportation agencies to assess pavement conditions. The two papers in this thesis evaluated the uncertainties associated with interpreting data from these devices and assessed potential applications.

In the first paper, FWD tests were conducted on asphalt pavements with varying supporting conditions, and individual layer modulus values were estimated using forward- and back-calculation methods. Dynamic cone penetrometer (DCP) test device was used to independently measure individual layer penetration resistance (PR) values to compare with the estimate moduli values. Results indicated that the predicted subgrade moduli values from forward- and back-calculations are strongly correlated but produce slightly different values. The predicted asphalt and base layer moduli values from forward- and back-calculations, however, showed significant scatter. Comparison between DCP-PR and the predicted base and subgrade layer modulus yielded non-linear relationships. The relationships produced lower standard errors when only data from subgrade layer is considered. The relationships developed in this study fell within the upper and lower bounds of relationships documented in the literature.

In the second paper, the efficacy of using a ground-coupled GPR system and a hand-held dielectric property measurement device to determine the asphalt and pavement foundation layer thicknesses is assessed. The actual pavement thicknesses were measured from pavement cores and foundation layer thicknesses were obtained using dynamic cone penetrometer (DCP) tests. Further, the viability of using GPR to detect moisture variations in the base layers is assessed. Tests were conducted on various asphalt pavement test sections

built at a test site in Iowa with different foundation support and drainage conditions, and layer thicknesses. A comparative analysis of core measurements and asphalt thickness estimated from GPR showed a 10% average error. Base layer thicknesses could not be evaluated using GPR data due to variations in moisture contents. Based on the dielectric properties calculated from GPR scans, the estimated moisture contents in the base layer varied from about 5 to 15%. The variations in moisture contents between the test sections are attributed to variations in gradation and permeability properties of the base layer.

CHAPTER 1. INTRODUCTION

This chapter is organized into sections that present the research problem, the research goals and objectives, and a discussion of the significance of this research. The final section describes the chapter organization of this thesis.

Research Problem

To assess pavement and foundation layer properties, falling weight deflectometer (FWD) and ground penetrating radar (GPR) nondestructive testing (NDT) methods are being increasingly used in tandem by highway agencies. FWD is used to measure pavement and foundation layer moduli values with inputs of layer thicknesses obtained from GPR measurements. Dynamic cone penetrometer (DCP) is an intrusive testing method that is also commonly used to determine layer thicknesses and empirically estimate foundation layer strength and moduli values.

To determine layer moduli values, FWD data analysis requires either forward- or back-calculation analysis. Forward calculations involve using deflection basin measurements in closed-loop equations. Back-calculations involve selecting initial moduli values for each layer and modifying them in an iterative process until the predicted deflection basin matches the measured deflection basin. There are many forward- and back-calculation methods that have been documented in the literature and each method has its own advantages and disadvantages (Smith et al. 2007; Stubstad et al. 2007). Some previous studies have documented empirical relationships between back-calculated FWD moduli values and DCP test measurements. However, the influence of the calculation procedure followed in FWD analysis on the empirical relationships is not well documented. This is important to understand as many agencies rely on those empirical relationships in pavement design.

In order to determine layer thicknesses from GPR data, dielectric constant properties of layers are typically assumed based on published values in literature. However, the dielectric properties of materials can vary with moisture content at the time testing, material type, and curing time if stabilizing admixtures such as cement or fly ash are used, and ground temperatures (i.e., frozen or unfrozen). Accurate determination of layer thickness is important in FWD data analysis and also in quality control/quality assurance testing conducted to evaluate if target thicknesses are achieved during construction.

Goal of The Research

The main goal of this research is to explore how FWD and GPR nondestructive testing can be used to accurately and reliably determine pavement and foundation layer properties for quality control/assurance and performance assessment. To achieve this goal, this research is divided into two topics: (A) evaluating relationships between individual moduli values determined from FWD deflection data and layer properties determined from DCP, and (B) assessing dielectric properties of pavement and foundation layers in layer thickness and foundation moisture content estimation using GPR.

Objectives

The specific objectives for the FWD data analysis are as follows:

- Conduct FWD testing on asphalt pavements with different support conditions (i.e., stabilized and unstabilized) to determine individual layer moduli values.
- Conduct DCP testing to determine individual layer properties and layer thicknesses.
- Compare penetration resistance (PR) values obtained from DCP testing with individual layer FWD moduli values calculated using the following procedures:

    - Forward-calculation methods described by Stubstad et al. (2007) to calculate base/subbase and pavement layer moduli values.
    - Back-calculation analysis for flexible pavements using Engineering Research Institute data analysis (ERIDA) software. (Engineering and Research International Inc. 2009)
- Compare the FWD moduli vs. DCP-PR relationships with published empirical relationships.

Specific research objectives for GPR data analysis are as follows:

- Conduct laboratory testing to determine dielectric properties of cohesive (stabilized and unstabilized) and granular materials at various compaction moisture contents in as-compacted and frozen states, using a hand-held device called GS3 manufactured by Decagon Devices, Inc.
- Compare dielectric properties determined by GS3 hand-held device and back-calculated dielectric properties from GPR readings.
- Conduct field GPR scans on asphalt pavement sections to determine the viability of using laboratory determined dielectric properties in accurately determining pavement and base layer thickness.

Significance of The Research

The two research articles will help transportation agencies, contractors, and researchers understand the factors that affect layer moduli and thickness values determined from FWD and GPR data. The first paper fills a gap in the research in two ways, first by reporting the influence of the different analysis methods used in determining the in situ moduli values and the statistical relationships between the methods based on a large dataset, and second, by

examining the uncertainty of using DCP penetration resistance values to predict in situ layer moduli values. The second paper challenges the common practice of using a single dielectric constant value in GPR thickness calculations of complex in situ pavement foundation properties and also use GPR as a nondestructive method to estimate in situ foundation layer moisture content. This approach provides a new way to potentially evaluate foundation drainage condition.

Organization of The Document

Following this introductory chapter, the thesis is organized into four additional chapters. Chapter 2 is a paper, "Estimating in Situ Modulus Using Falling Weight Deflectometer and Dynamic Cone Penetrometer," that will be submitted to *Transportation Geotechnics*. Chapter 3 is paper, "Assessing Pavement and Foundation Properties by Using Ground Penetrating Radar," that will be submitted to *Nondestructive Testing and Evaluation*. Chapter 4 summarizes the conclusions and recommendations for future research and practice. A list of referenced works are provided at the end of each chapter.

Key Terms

FWD, GPR, nondestructive testing, flexible pavement, modulus, dielectric constant, lay thickness.

References

Engineering and Research International Inc. (2009). "ERI Data Analysis Users Guide: Version 7." Engineering and Research International, Inc., Savoy, IL.

Smith, K. D., Wade, M. J., and Bruinsma, J. E. (2007). "Using Falling Weight Deflectometer Data with Mechanistic-Empirical Design and Analysis-Draft Interim Report." Federal Highway Administration Office of Acquisition Management, Washington DC.

Stubstad, R., Jiang, Y. J., and Lukanen, E. (2007). "Forwardcalculation of Pavement Moduli with Load-Deflection Data." *Transportation Research Record: Journal of the Transportation Research Board*, 2005(1), 104-111.

CHAPTER 2. ESTIMATING IN SITU MODULUS USING FALLING WEIGHT DEFLECTOMETER AND DYNAMIC CONE PENETROMETER

A paper to be submitted to *Transportation Geotechnics*

Pavana K. R. Vennapusa, Jinhui Hu, and David J. White

Abstract

Falling weight deflectometer (FWD) test is routinely used by highway agencies to assess pavement conditions in situ. Deflection data from FWD tests is used to calculate layer moduli values using forward- or back-calculation methods. Many highway agencies also use empirical relationships to estimate modulus from dynamic cone penetrometer (DCP) penetration resistance (PR) values. In this paper, the influence of the calculation procedure used in estimating the moduli values and the uncertainties involved with the empirical relationships are assessed. FWD and DCP tests were conducted on 16 asphalt pavement test sections with varying age, supporting conditions, and pavement layer thicknesses. Forward-calculations recommended by Stubstad et al. (2007) and back-calculations using Engineering Research Institute data analysis software were used to determine pavement, subgrade, and intermediate (base) layer moduli values. Results indicated that the predicted subgrade moduli values from forward- and back-calculations are strongly correlated but produce values that vary on average by about 20%. The predicted asphalt and base layer moduli values from forward- and back-calculations, however, showed significant scatter. The standard error in the estimated moduli value was over 120 MPa for the base layer and 3,000 MPa for the asphalt layer. Comparison between DCP-PR and the predicted base and subgrade layer modulus yielded non-linear relationships with standard errors varying between 25 and 60 MPa. The standard errors decrease to about 10 to 17 MPa, when only data from subgrade

layer is considered (i.e., PR > 20 mm/blow). The relationships developed in this study fell within the upper and lower bounds of relationships documented in the literature.

Introduction

The mechanistic empirical pavement design guide (MEPDG) emphasizes the importance of proper characterization of pavement foundation layer mechanistic properties (e.g., modulus) for pavement analysis, design, and construction quality control/assurance (AASHTO 2008). Resilient modulus (M_r) for unbound foundation layers and elastic modulus (E) for bound foundation layers is a required input in the design and it has a significant effect on the computed pavement responses (Rao et al. 2012). Determining M_r through laboratory testing following AASHTO T-307 (AASHTO 2000) or NCHRP 1-28A (Andrei et al. 2004) testing protocols is suggested in the design guide for Level 1 analysis on newly constructed foundation layers. For Level 1 analysis on rehabilitation projects, backcalculated moduli values from falling weight deflectometer (FWD) testing per ASTM D4694-09 (ASTM 2009) is indicated as the preferred method in the design guide. For Level 2 analysis on new and rehabilitated projects, empirical relationships are used to determine the moduli values from California bearing ratio (CBR), penetration resistance (PR) values determined from dynamic cone penetrometer (DCP), and R-value (NCHRP 2004).

Use of FWD in estimating the modulus has advantages with the test being relatively rapid and non-destructive, and many state agencies are currently equipped with the test devices and are routinely using it as part of their asset management programs (Alavi et al. 2008). To determine layer moduli values, FWD data analysis requires either forward- or back-calculations. Forward-calculations involve using deflection basin measurements in closed-loop equations to determine the layer moduli values (Stubstad et al. 2007). Back-calculations

involve selecting initial moduli values for each layer and modifying them in an iterative process until the predicted deflection basin matches the measured deflection basin. There are many forward- and back-calculation methods that have been documented in the literature over the past three decades and each method has its own advantages and disadvantages (Smith et al. 2007).

Despite significant research and development over the past four decades on backcalculation analysis programs, many researchers have expressed challenges associated with the analysis procedures. The MEPDG (AASHTO 2008) acknowledges these challenges and states the following:

> "Backcalculation programs that use this iterative technique do not result in a unique solution or set of layer moduli. As such, determining a set of elastic layer moduli to match a measured deflection basin that deviates from elastic theory, for whatever reason, may become difficult and frustrating…… There are forward calculation programs that do result in unique layer moduli, but these have not been commonly used and are restricted to three layer structures."

Stubstad et al. (2006) stated that "a serious drawback to [backcalculation] is that one or more of the many input assumptions……may be incorrect and therefore may not apply to the actual pavement system……forward calculation is easy to understand and use, whereas backcalculation is presently more of an art than a science."

On the other hand, using other tests such as DCP to estimate modulus using empirical relationships also present significant uncertainty in the predicted values due to variations in material types and conditions, differences in test and analysis methods used in determining moduli values, and the scatter observed within those correlations. Review of literature

indicated that researchers have used laboratory triaxial (or resilient modulus) tests, FWD, static or cyclic plate load tests, and laboratory or field small-strain wave propagation tests (Chen et al. 2005; George and Uddin 2000; Heukelom and Klomp 1962; Mohammad et al. 2007; Powell et al. 1984). Even between the correlations studies that involved FWD tests to determine moduli values, different calculation procedures were used in the analysis. The influence of the backcalculation or forward calculation procedure followed in FWD analysis on the empirical relationships is not well documented in the literature. This is important to understand as many agencies rely on such empirical relationships in their pavement design.

This study was undertaken with the goal of understanding the uncertainties involved in estimating the flexible pavement and foundation layer moduli values using FWD and DCP. Testing was conducted on 16 asphalt pavement test sections in Hamilton and Boone Counties in Iowa with varying pavement age, support conditions, and foundation layer thicknesses. Modulus values of asphalt, subgrade, and intermediate base layers were determined from FWD data using forward-calculations recommended by Stubstad et al. (2007) and back-calculations using Engineering Research Institute data analysis software.

FWD Testing and Data Analysis Procedures

FWD testing involves dropping a weight on a circular plate and measurement deflections directly beneath the plate and at several locations away from the plate. MEPDG recommends the FWD test be performed in accordance with ASTM D4694-09 standard (ASTM 2009). A typical FWD plate and deflection sensor setup and a deflection basin for sensor setup used on flexible pavements is shown in Figure 2.1.

The data obtained from the deflection basin for a given load is analyzed using either forward or backcalculation methods. A detailed overview of all the forward and

backcalculation methods is provided elsewhere in the literature (Irwin 2002; Smith et al. 2007; Stubstad et al. 2006; Von Quintus and Simpson 2002). In the following sections, an overview of the forward calculation methods followed in this study as proposed by Stubstad et al. (2007) and the backcalculation analysis procedure followed in this study using the Engineering Research International Data Analysis (ERIDA) software are provided.

Forward Calculation Methods

AASHTO Method for Subgrade Modulus Determination

AASHTO (1993) presents simple closed-form equations based on Boussinesq solutions to determine subgrade moduli values. The original Boussinesq equations relating vertical deflection, applied stress, and elastic modulus for load applied at the surface of a half-space elastic, homogenous, and isotropic material are expressed as:

$$E = (1 - v^2)Pf/(\pi a d_o) \text{ for uniformly distributed load at r = 0} \quad (1)$$

$$E = (1 - v^2)P/(\pi r d_r) \text{ for point load on the surface at any r} \quad (2)$$

where,

E = Elastic modulus (MPa);

P = applied load (N);

r = distance of deflection reading d_r from center of load (mm);

d_r = deformation at a distance r from the center of the load (mm);

d_o = deformation at the center of the loading plate (mm);

v = Poisson's ratio; and

f = shape factor that depends on the rigidity of the plate and the material type (i.e., cohesive or granular or mixed) and varies between $\pi/2$ to 8/3, depending on the anticipated stress distribution (Vennapusa and White 2009).

Eq.1 uses deformation directly beneath the loading plate, which is a composite measure of all layers within its measurement influence depth, and therefore represents a composite modulus of the material. Ullitdtz (1987) indicated that the *E* values calculated using Eq.2 represent the subgrade modulus, provided the distance *r* is sufficiently large such that there is no influence of deformation of the layers above the subgrade. AASHTO (1993) describes a relationship to determine the minimum distance *r*, based on Odemark's method of equivalent layer thickness (MET) method (Odemark 1949) combined with the Boussinesq's solutions. The MET method is described in detail in Ullidtz (1987).

Ullitdz (1987) indicated that if E values determined from Eq.1 and 2 are plotted against distance *r*, using deflections obtained at various distances away from the plate, one of the following two trends are generally observed: (1) modulus decreases with increasing distance and then levels off after a certain distance or (2) modulus initially decreases and then increases after a certain distance. The first type of trend reportedly represents a linear elastic subgrade and the lowest modulus value can be used as the subgrade modulus value. The second type of trend represents a non-linear subgrade indicating stress-dependency. For this case, according to Salt (1998) the lowest modulus value calculated can be used as the subgrade modulus value. Ullidtz (1987) proposed a stress-dependent non-linear model to address this case, but it requires an iterative procedure to determine the curve fitting parameters in the non-linear model. Some software programs (e.g. ELMOD developed by Dynatest, Inc.) currently use the nonlinear model in subgrade analysis.

Hogg Model for Subgrade Modulus Determination

The Hogg model is described in detail by Stubstad et al. Stubstad et al. (2007), Hogg et al. (1944) developed the original model based on a hypothetical two-layer pavement

system. This model simplifies multilayered elastic system to calculate subgrade stiffness, and elastic modulus under a surface load. The Hogg model as modified by Wiseman and Greenstein (1983) was used in this study. The model consist of a series of equations to compute subgrade layer modulus as follows:

$$E = I\frac{(1+v)(3-4v)}{2(1-v)}\left(\frac{S_0}{S}\right)\left(\frac{p}{\Delta_0 l}\right) \tag{3}$$

$$l = y_0\frac{r_{50}}{2} + [(y_0 r_{50})^2 - 4mar_{50}]^{1/2} \qquad if\ \frac{a}{l} < 0.2, then\ l = (y_0 - 0.2m)r_{50} \tag{4}$$

$$r_{50} = r\frac{\left(\frac{1}{\alpha}\right)^{\frac{1}{\beta}} - B}{\left[\frac{1}{\alpha}\left(\frac{d_0}{d_r} - 1\right)\right]^{\frac{1}{\beta}} - B} \tag{5}$$

$$\left(\frac{S_0}{S}\right) = 1 - \overline{m}\left(\frac{a}{l} - 0.2\right) \qquad if\ \frac{a}{l} < 0.2, then\ \frac{S_0}{S} = 1 \tag{6}$$

where,

v = Poisson's ratio for subgrade

S_0 = Theoretical point load stiffness

S = Pavement stiffness calculated as P/d_0 (area loading)

P = Applied load

d_0 = Deflection at center of load plate

d_r = Deflection at offset distance r

r = Distance from center of load plate

r_{50} = Offset distance where $\Delta_r/\Delta_0 = 0.5$

l = Characteristic length

α, β, B = Curve fitting coefficients (see Table 2.1)

y_0, m = Characteristic length coefficients (see Table 2.1)

$\overline{m}$ = Stiffness ratio coefficient (see)

The Hogg model described by Wiseman and Greenstein (1983) included three cases: Cases I and II are used for finite elastic layer with an effective thickness which is assumed to be 10 times of the characteristic length *l* and Case III is an infinite elastic foundation. The difference between Cases I and II are the assumed Poisson's ratio which is 0.5 for Case I and 0.4 for Case II. According to Stubstad et al (2007), Case II is typically used in calculating subgrade layer moduli and provides conservative values. The model coefficients for Case II are summarized in Table 2.1.

AREA Forward Calculation Method for Asphalt Surface Layer Modulus Determination

The AREA method was defined in Hoffman and Thompson (1981) and is commonly used in rigid pavement analysis. Stubstad et al. (2006) proposed a simple set of equations using the AREA method for determining asphalt surface layer moduli values based on calibrations carried out with multi-layered elastic analysis programs. The procedure requires calculation of AREA factor (AF), composite modulus using Eq.1, and normalized surface layer thickness to the loading plate. The following equations are used to calculate asphalt pavement modulus:

$$E_{AC} = \left[E_0 * AF_{AC} * k_3^{\left(\frac{1}{AF_{ac}}\right)}\right] / k_3^2 \tag{7}$$

$$AF = \left[(k_2 - 1)/(k_2 - \frac{A_{12}}{k_1})\right]^{1.35} \tag{8}$$

$$A_{12} = 2 * [2 + 3\left(\frac{d_8}{d_0}\right) + \left(\frac{d_{12}}{d_0}\right)] \tag{9}$$

where,

E_{AC} = modulus of the asphalt layer;

E_0 = composite modulus of the entire pavement system calculated using Eq.1;

AF = AREA factor;

k_1 = 6.85

k_2 = 1.752

k_3 = thickness ratio of upper layer thickness / load plate diameter = h_1 / (2*a);

a = radius of the load plate;

h_1 = thickness of the asphalt layer;

A_{12} = AREA beneath the first 305 mm (12 in.) of the deflection basin;

d_0 = deflection measured at the center of the loading plate;

d_8 = deflection measured at 203 mm (8 in.) away from the center of the plate; and

d_{12} = deflection measured at 305 mm (12 in.) from the center of the plate.

According to Stubstad et al. (2007), these equations work very well for typical pavement materials and modular ratios when the underlying materials are unbound. It is also noted therein that this approach is not totally rigorous but is rather empirical in nature.

Dorman and Metcalf Forward Calculation Method for Base Layer Modulus Determination

Stubstad et al. (2007) proposed using the Dorman and Metcalf (1965) method to determine modulus intermediate (base) layer between the bound surface and unbound subgrade layers. Equation 10 is used to calculate the base layer modulus:

$$\mathrm{E_{Base}} = 0.86 \times \mathrm{h_2^{0.45}} \times \mathrm{E_{SG}} \qquad (10)$$

where,

E_{Base} = base layer modulus (psi);

h_2 = Thickness of the base layer (in.); and

E_{SG} = Subgrade modulus (psi).

According to Stubstad et al. (2007), the above method provides reasonable and realistic base course modulus.

ERIDA Backcalculation Method

ERIDA backcalculation software is provided by Engineering Research International, Inc. (2009). This method assumes that the surface load is uniformly distributed over a circular area; all layers are homogenous, isotropic, and linearly elastic; upper layers extend horizontally to infinity; and bottom layer is a semi-infinite half-space. ERIDA uses the ELSYM5 calculation routine in analyzing pavement deflections. Details of ELSYM 5 calculation routine are provided in Ahlbornm (1972). The process requires inputting a seed (or initial) modulus for each layer, the lower and upper bounds of modulus for each layer, Poisson's ratio of each layer, and thicknes of each layer. The ERIDA software uses an iterative approach where the layer moduli are repeatedly adjusted until a suitable match between the calculated and measured deflection basin is found. The program computes the root mean square error (RMSE) between the measured and the calculated deflection values and runs the iterations until the lowest RMSE is achieved. Review of literature indicated that acceptable errors in backcalculation vary from 2% to 10% (Cole and Kolluri 2008; Engineering and Research International Inc. 2009; Hawks et al. 1993). AASHTO (2008) indicates that RMSE > 3% generally implies that the modulus values calculated are questionable. Irwin (2002) indicated that although RMSE is advisable to check the deflection basin fit, it does not assure that the backcalculated modulus values are "correct."

DCP Testing and Empirical Relationships to Determine Modulus

DCP testing involves dropping an 8 kg hammer mass from a drop height of about 574 mm and measuring the penetration depth of a penetrating rod attached to a cone. The test procedure is described in ASTM D6951-03 (ASTM 2003). The standard provides the following equations to estimate CBR from PR values:

$CBR = \frac{292}{PR^{1.12}}$ for all soils except lean clays with CBR < 10 and high plasticity clays (11)

$$CBR = \frac{1}{(0.017019 \times PR)^2} \text{ for lean clays with CBR < 10} \quad (12)$$

$$\text{CBR} = \frac{1}{0.002871 \times \text{PR}} \text{ for high plasticity clays} \quad (13)$$

where,

PR = Penetration resistance (mm/blow).

Many researchers have developed empirical relationships to estimate modulus values for foundation layers from PR and CBR measurements. A summary of those relationships is provided in Table 2.2 along with the statistical parameters (i.e., coefficient of determination R^2, standard error (SE) associated with the relationships and their validity ranges. The R^2 values of the relationships ranged from about 0.4 to 0.9. In these relationships, the procedures used to determine the modulus values included both laboratory and field testing methods. FWD was the most commonly used method to determine the modulus values using backcalculation analysis. Various different backcalculation analysis procedures were used as summarized in Table 2.2. In this study, forward and backcalculation methods were used to estimate E and correlate with PR measurements.

Figure 2.2 shows the upper and lower bounds of relationships between PR and elastic or resilient modulus values documented in the literature and summarized in Table 2.2. The bounds suggest that the predicted moduli values can have an error of ± 50 to 335 MPa if PR value is between 2 and 10 mm/blow, and ± 5 to 50 MPa if PR value is > 10 mm/blow. Relationships obtained from this study are also included in Figure 2.2, and will be discussed below.

In MEDPG, the empirical relationship provided by Powell et al. (1984) between CBR and E is used as default, where CBR are estimated from DCP-PR values using Eq.11. The E value determined from Powell et al. (1984) equation is assumed to be same as M_r in MEPDG (NCHRP 2004).

Field Data Collection and Data Analysis

Description of Test Sites

The test sections are located in Hamilton County (County Road D65, 320th Street, Queens Avenue, Vail Ave, and County Road D20) and Boone counties (Boone Expo 1st Street to 11th Street) in Iowa. Hamilton County D65 test section was the oldest pavement with multiple asphalt pavement layers constructed from 1959 to 2001 as overlays and exhibited transverse and longitudinal cracking on the surface. The remaining pavement sections were constructed between 2006 and 2013 and did not have any visible distresses at the surface. This information and testing dates are summarized in Table 2.3.

The pavement sections varied in surface layer thicknesses from 101 to 203 mm and base/subbase layer thicknesses from 152 to 457 mm. Material index properties of the subbase and subgrade layers from some of the project sites are summarized in Table 2.4. The Hamilton County test sections consisted of multiple base/subbase layers (i.e., choke stone, modified subbase, road stone, and macadam subbase). Properties of materials obtained from the D20 site are included in Table 2.4. According to the County Engineer, the materials with similar descriptions on the other sites were similar to materials used at the D20 site. Material properties of rolled stone base at the D65 and MSB layer at the 320th St. and Queens Ave. sites were not available. According to the County Engineer, the MSB layers confirmed to

Iowa DOT MSB gradation and similar material was used at the Boone Expo site and the properties are summarized in Table 2.4.

The Boone Expo site consisted of various test sections built as part of an on-going research study. The foundation layer construction details are summarized in White et al. (2012). In brief, all test sections are surfaced with a nominal 152 mm thick hot mix asphalt (HMA) or warm mix asphalt (WMA) layer underlain by a nominal 152 mm thick crushed limestone MSB layer. Geocells are used within the MSB layer on 3rd street, and geotextiles and geogrids were used at the MSB layer and subgrade layer interface on 3rd, 4th, and 5th street sections. 1st, 3rd, 4th, 5th, 8th, and 10th streets consisted of natural or compacted subgrade layer directly beneath the MSB layer. On 2nd, 7th, 9th, and 11th streets, either an untreated or treated subbase/subgrade layer was used between the MSB and subgrade layers, as summarized in Table 2.3.

Field Testing

In this study, a KUAB FWD setup with the plate and sensor setup shown in Figure 2.1 was used. Testing was conducted and deflections were measured in accordance with ASTM (2009). The pavement surface temperature and the pavement layer temperatures were obtained at various depths to determine the asphalt mix temperature to correct the deflections obtained beneath the plate, according to AASHTO (1993).

FWD testing was conducted on Hamilton County test sites at about 120 test locations at three different times (August 2012, April 2013 during spring-thaw in Iowa, and September 2013) to capture seasonal variations in the moduli values. For FWD testing on D65, care was taken such that none of the sensors were close to (within in 0.5 m) of the cracks present on

the surface. FWD testing conducted at different times, were conducted at the same test locations.

FWD and DCP testing was conducted on Boone County test sections in April 2013 during spring-thaw in Iowa. FWD tests were conducted at 101 test locations while DCP tests were conducted at 36 selected test locations representing the range of foundation support conditions on this site.

DCP tests were conducted in accordance with ASTM D 6951-03 (ASTM 2003), directly on the base layer by removing a 150 mm diameter core from the pavement surface. Tests were conducted using a 900 mm long penetrating rod.

Data Analysis

FWD data was used to calculate the composite moduli values using Eq.1, and are reported as $E_{FWD\text{-}Composite}$. Forward and backcalculation of FWD deflection basin data was performed to determine the subgrade, asphalt surface, and intermediate base layer moduli values, using the procedures described earlier in this paper. Subgrade modulus calculated using the AASHTO method are reported as $E_{FWD\text{-}AASHTO\text{-}SG}$ values (Eq.2). Subgrade modulus calculated using the Hogg method (Case II) are reported as $E_{FWD\text{-}Hogg\text{-}SG}$ values (Eq.3). The asphalt surface layer modulus calculated using the AREA method are reported as $E_{FWD\text{-}AREA\text{-}Asphalt}$ values (Eq.7). The intermediate base layer modulus calculated using $E_{FWD\text{-}AASHTO\text{-}SG}$ and $E_{FWD\text{-}Hogg\text{-}SG}$ as E_{SG} values in Eq.10 and are reported as $E_{FWD\text{-}AASHTO\text{-}Base}$ and $E_{FWD\text{-}Hogg\text{-}Base}$, respectively. The backcalculated layer moduli values obtained using ERIDA are reported as $E_{FWD\text{-}ERI\text{-}Asphalt}$ for asphalt layer modulus, $E_{FWD\text{-}ERI\text{-}Base}$ for base layer modulus, and $E_{FWD\text{-}ERI\text{-}SG}$ for subgrade layer modulus.

For all pavement sections, the multiple base/subbase layers were combined into one base layer to simplify the analysis into a three-layer system. This decision was made after reviewing the DCP-PR profiles from the Boone test sections, which showed that the base/subbase layers yielded similar PR values compared to the underlying subgrade layer. Representative PR profiles from selected test sections at the Boone expo site are shown in Figure 2.3. Some test points on 7th street and 11th street north reached refusal (i.e., < 2 mm after 5 blows, per ASTM D6951-03) within the chemically stabilized subbase/subgrade layers. PR from those test points were not determined for this study.

On the 11th street north section with PC or FA stabilized subgrade between the MSB and subgrade layers, the calculations showed unreasonably high moduli values using the ERIDA backcalculation method when the MSB and stabilized subgrade layers were analyzed as separate layers (four-layer system). As the MSB and the PC stabilized subgrade layers showed similar PR values (see Figure 2.3 for 11th St. N section results), the two layers were combined and analyzed as a single base layer (three-layer system) in both forward- and back-calculations.

Layer thicknesses from the Boone expo sections were obtained from DCP testing, while design thicknesses were used for Hamilton County test sections. The thicknesses were determined using DCP test results as illustrated in Figure 2.3. The base layer thickness was determined as the depth from the bottom of the asphalt layer to the intersection of the tangents of the upper and lower portions of the cumulative blows with depth curve.

In both forward- and back-calculations, a Poisson's ratio of 0.45 was assumed for subgrade and 0.4 for base and 0.35 for asphalt layers.

In backcalculation analysis, RMSE ≤ 3.0 was used as the criteria in determining the layer moduli values, in accordance with AASHTO (2008). This criteria could not be achieved for a few data points, and those data points were excluded from the analysis.

In determining the PR of each layer, the thickness of each layer divided by the cumulative blows needed for the cone tip to reach that depth was used. This procedure was straight-forward for base layer, where the thickness was easily distinguishable. For the subgrade, the PR values varied with depth (Figure 2.3). Therefore, PR representing the average of the top 300 mm of the subgrade and PR representing the weakest 75 mm thickness within the DCP penetration depth were calculated for comparison with the modulus values. The weakest layer approach was found to work well in correlating with FWD backcalculated modulus of subgrade reaction values in a recent study conducted by White and Vennapusa (2014).

Results and Discussion

Average composite FWD moduli values from all test sections are shown in Figure 2.4 which ranged between 300 to 950 MPa. Tests from multiple testing times on Hamilton County test sections indicated that the composite moduli values decreased during the spring-thaw time, as expected.

Figure 2.5 and Figure 2.6 shows the average base and subgrade layer moduli values, calculated using the forward- and back-calculation methods from each test section and the testing time. Statistical regression analysis between the forward and backcalculated subgrade moduli values from all test points are shown in Figure 2.7. Similarly, regression analysis results for base layer and surface layer moduli values are shown in Figure 2.8 and Figure 2.9, respectively.

On average, the AASHTO method produced the highest and the Hogg method produced the lowest subgrade moduli values. The back-calculation method produced average subgrade moduli values that are in between the two forward-calculation methods. Stubstad et al. (2006) indicated that Hogg method typically produces conservative (lower) subgrade moduli values, which was also the case for the results presented herein. The R^2 values of the regression relationships between the subgrade moduli values estimated from the three methods ranged from 0.85 to 0.95. On average, the AASHTO and ERIDA methods produced subgrade moduli values that are about 1.3 and 1.5 times higher than the Hogg method.

Base layer modulus calculations showed significant variations between the forward- and backcalculation methods. On average, the base layer moduli values calculated based on the subgrade moduli values form Hogg method produced the lowest moduli values. Regression relationships between the forward- and back-calculated moduli values yielded low R^2 values (< 0.3) and high SE values (> 120 MPa). The R^2 value for the two forward calculation methods was high (> 0.90) and about the same as in the case of subgrade modulus calculations. This was expected because the same Dorman and Metcalf method was followed in calculating the base layer moduli for both cases.

In surface asphalt layer modulus calculations, the regression analysis between the backcalculated and forward calculated methods yielded a best fit line close to the 1:1 line with $R^2 = 0.65$, although there the SE was about 3,000 MPa. Regression equation presented in Stubstad et al. (2007) comparing back- and forward-calculation methods based on 1300 test points obtained from long term pavement performance (LTPP) test sections is also shown in Figure 2.9, for reference. It must be noted that the back-calculated values presented in Stubstad et al. (2007) used MODCOMP backcalculation program Stubstad et al. (2006).

Figure 2.10 shows the relationships between PR and base and subgrade layer moduli values, based on testing conducted at the Boone Expo test site. Figure 2.10 (a), (b), (c) shows the PR values of the subgrade using the 75 mm thick weakest portion of subgrade, and Figure 2.10 (d), (e), (f) shows PR values of the subgrade using the top 300 mm subgrade. The data included PR values ranging between 2 and 78 mm/blow.

The relationships between PR and moduli values yielded non-linear exponential relationships, similar to presented by others as summarized in Table 2.2. The forward-calculation methods yielded slightly higher R^2 values and lower SE values, compared to the backcalculation method. The PR values determined from the weakest 75 mm of the subgrade produced slightly higher R^2 values (R^2 = 0.57 to 0.59) than with PR values determined from the top 300 mm of the subgrade (R^2 = 0.46 to 0.54). When only data from the subgrade with PR > 23 mm/blow are considered, the SE of the estimates reduced to < 20 MPa, although the R^2 values are also low (< 0.1).

Key Findings and Conclusions

The key findings and conclusions from this study are as follows:

- The AASHTO and Hogg forward calculation methods and ERIDA backcalculation program produced subgrade moduli values that are strongly correlated with R^2 between 0.85 and 0.95 and SE < 13 MPa. However, the AASHTO and ERIDA methods produced subgrade moduli values that are 1.28 and 1.51 times higher than the Hogg method.
- Base layer modulus calculations showed significant variations between the Dorman and Metcalf forward calculation and the ERIDA back calculation method. Regression

relationships between forward and backcalculated moduli values yielded low R^2 values (< 0.3) and high SE values (> 120 MPa).

- Regression analysis between the backcalculated and forward calculated asphalt layer moduli values yielded a linear relationship that is close to the 1:1 line with $R^2 = 0.65$. However, there was significant scatter in the data with a SE of about 3,000 MPa.
- Numerous regression relationships have been documented in the literature between DCP test measurements and moduli values and are summarized in this paper. Upper and lower bounds are presented based on the available relationships. The bounds suggest that the predicted moduli values can have an error of ± 50 to 335 MPa if PR value is between 2 and 10 mm/blow, and ± 5 to 50 MPa if PR value is > 10 mm/blow.
- New relationships between PR and moduli values calculated from three forward and back calculation methods for a PR range of 2 and 78 mm/blow are presented in this paper. PR values determined from the weakest 75 mm of the subgrade showed slightly higher R^2 values when compared to PR values for the top 300 mm of the subgrade.
- The relationships presented in this study indicated that for if data over PR = 2 to 78 mm are considered, the SE of the estimate ranged from 24 to 60 MPa, depending on the modulus calculation method. The SE of the estimate decreased to < 20 MPa, when data from PR = 23 to 78 (i.e., only subgrade) are considered.

References

AASHTO (1993). *AASHTO guide for design of pavement structures 1993*, American Association of State Highway and Transportation Officials, Washington, D.C.

AASHTO (2000). *Determining the resilient modulus of soils and aggregate materials*, American Association of State Highway and Transportation Officials T-307 Laboratory Resilient modulus Tests, Washington, D.C.

AASHTO (2008). *Mechanistic-Empirical Pavement Design Guide: A Manual of Practice*, American Association of State Highway Officials and Transportation Officials, Washington, D.C.

Ahlbornm, G. (1972). "ELSYM5, Computer Program for Determining Stresses and Deformations in Five Layered Systems." University of California, Berkeley.

Alavi, S., LeCates, J. F., and Tavares, M. P. (2008). "Falling Weight Deflectometer Usage." Transportation Research Record: Journal of the Transportation Research Board, Washington, DC.

Andrei, D., Witczak, M. W., Schwartz, C. W., and Uzan, J. (2004). "Harmonized Resilient Modulus Test Method for Unbound Pavement Materials." *Transportation Research Record: Journal of the Transportation Research Board*, 1874(1), 29–37.

ASTM (2003). "ASTM D6951 - 03 Standard Test Method for Use of the Dynamic Cone Penetrometer in Shallow Pavement Applications." <http://www.astm.org/DATABASE.CART/HISTORICAL/D6951-03.htm>. (April 18, 2015).

ASTM (2009). "ASTM D4694-09, Standard Test Method for Deflections with a Falling-Weight-Type Impulse Load Device."

Chen, D.-H., Lin, D.-F., Liau, P.-H., and Bilyeu, J. (2005). "A correlation between dynamic cone penetrometer values and pavement layer moduli." *Geotechnical Testing Journal*, 28(1), 42-49.

Chen, J., Hossain, M., and LaTorella, T. M. (1999). "Use of falling weight deflectometer and dynamic cone penetrometer in pavement evaluation." *Transportation Research Record*(1655), p. 145-151.

Cole, D., and Kolluri, K. (2008). *Mechanistic-Empirical Pavement Design Guide, Interim Edition: A Manual of Practice*, American Association of State Highway and Transportation Officials, Washington, D.C.

De Beer, M. (1990). "Use of the Dynamic Cone Penetrometer (DCP) in the Design of Road Structures." 167-176.

Dorman, G. M., and Metcalf, C. T. (1965). "Design Curves for Flexible Pavements Based on Layered System Theory." *Highway Research Record* 71, 69–84.

Engineering and Research International Inc. (2009). "ERI Data Analysis Users Guide: Version 7." Engineering and Research International, Inc., Savoy, IL.

George, K. P. (2004). "Prediction of Resilient Modulus from Soil Index Properties."University of Mississippi, 72.

George, K. P., and Uddin, W. (2000). "Subgrade Characterization for Highway Design." Mississippi Department of Transportation Research Division, Jackson, MS.

Hawks, N., F.,, Richter, C. A., Barrett, M., and Baker, C. (1993). "Falling Weight Deflectometer Relative Calibration Analysis." Strategic Highway Research Program National Academy of Science, Washington, DC.

Heukelom, W., and Klomp, A. (1962). "Dynamic Testing as A Means of Controlling Pavements During and After Construction." *International Conference on the Structural Design of Asphalt Pavements*, 203(1), 667-679.

Hoffman, M. S., and Thompson, M. R. (1981). "Mechanistic interpretation of nondestructive pavement testing deflections." Interim Report Illinois Univ., Urbana-Champaign. Dept. of Civil Engineering.

Hogg, A. H. A. (1944). "Equilibrium of a Thin Plate on an Elastic Foundation of Finite Depth." *The London, Edinburgh, and Dublin Philosophical Magazine and Journal of Science*, 35(243), 265–276.

Irwin, L. H. (2002). "Backcalculation: An overview and perspective." *Pavement Evaluation ConferenceRoanoke, Virginia, USA*.

Konard, J. M., and Lachance, D. (2001). "Use of in situ penetration tests in pavement evaluation." *Canadian geotechnical journal*, 38(5), 924-935.

Mohammad, L. N., Herath, A., Gaspard, K., Abu-Farsakh, M. Y., and Gudishala, R. (2007). "Prediction of Resilient Modulus of Cohesive Subgrade Soils from Dynamic Cone Penetrometer Test Parameters." *Journal of Materials in Civil Engineering*, 19(11), 986-992.

Nazzal, M. M. (2003). "Field evaluation of in-situ test technology for QC/QA procedures during construction of pavement layers and embankments " Master of Science, Birzeit University.

NCHRP (2004). "Guide for Mechanistic-Empirical Design of New Pavement and Rehabilitated Pavement Structures, Final Report, Part 2. Design Inputs Chapter 3. Material Characterization." National Cooperative Highway Research Program, Champaign, Illinois.

Odemark, N. (1949). "Investigations as to the Elastic Properties of Soils and Design of Pavements According to the Theory of Elasticity." Meddelande 77.

Pen, C. K. (1990). "An Assessment of the Available Methods of Analysis for Estimating the Elastic Moduli of Road Pavements." *Thrid International Conference on Bearing Capacity of Roads and Airfields*, Norwegian Institute of Technology, Trondheim, Norway.

Powell, W. D., Potter, J. F., Mayhew, H. C., and Nunn, M. E. (1984). "The structural design of bituminous roads." Transport and Road Research Laboratory, London.

Rao, C., Tutus-Clover, L., Bhattacharya, B., Darter, M. I., Stanley, M., and Von Quintus, H. L. (2012). "Estimation of Key PCC, Base, Subbase, and Pavement Engineering Properties from Routine Tests and Physical Characteristics." Federal Highway Administration, McLean, VA.

Salt, G. (1998). "Pavement Deflection Measurement and Interpretation for The Design of Rehabilitation Treatments." *Transit New Zealand Report*, 117.

Smith, K. D., Wade, M. J., and Bruinsma, J. E. (2007). "Using Falling Weight Deflectometer Data with Mechanistic-Empirical Design and Analysis-Draft Interim Report." Federal Highway Administration Office of Acquisition Management, Washington DC.

Stubstad, R., Jiang, Y. J., and Lukanen, E. (2007). "Forwardcalculation of Pavement Moduli with Load-Deflection Data." *Transportation Research Record: Journal of the Transportation Research Board*, 2005(1), 104-111.

Stubstad, R. N., Jiang, Y. J., and Lukanen, E. O. (2006). "*Guidelines for review and evaluation of backcalculation results*." Federal Highway Administration, Washington, D.C.

Ullidtz, P. (1987). *Pavement Analysis*, Developments in Civil Engineering Series, Elaevier, New York.

Vennapusa, P. K. R., and White, D. J. (2009). "Comparison of Light Weight Deflectometer Measurements for Pavement Foundation Materials." *ASTM geotechnical testing journal*, 32(3), 239-251.

Vennapusa, P. K. R., White, D. J., Siekmeier, J., and Embacher, R. A. (2012). "In situ mechanistic characterisations of granular pavement foundation layers." *International Journal of Pavement Engineering*, 13(1), 52-67.

Von Quintus, H. L., and Simpson , A. L. (2002). "Back-Calculation of Layer Parameters for LTPP Test Sections, Volume II: Layered Elastic Analysis for Flexible and Rigid Pavements." Federal Highway Administration, McLean, Virginia.

White, D. J., Vennapusa, P. K., Han, J., Christopher, B., Gieselman, H., Wang, S., Riko, W., Becker, P., Horhota, D., and Pokharel, S. (2012). "Compaction "Roadeo" Field Demonstration Project Report: Roller-Integrated Compaction Monitoring and Subgrade Geosynthetic Reinforcement." *SHRP 2 R02 Geotechnical Solutions for Soil Improvement, Rapid Embankment Construction, and Stabilization of the Pavement Working Platform*Washington, D.C., 140.

White, D. J., and Vennapusa, P. K. R. (2014). "Optimizing Pavement Base, Subbase, and Subgrade Layers for Cost and Performance of Local Roads." Iowa Highway Research Board; Iowa Department of Transportation, Iowa.

Wiseman, G., and Greenstein, J. (1983). "Comparison of Methods of Determining Pavement Parameters from Deflection Bowl Measurements." *Proceeding of the 7th Asian Regional Conference on Soil Mechanics and Foundation Engineering*, 158-165.

Table 2.1 Hogg model coefficients (modified from Stubstad et al. 2007)

Parameter	Coefficient	Values
Assumed depth to hard bottom	h/l	10
Poisson's ratio	V	0.40
"Influence" factor	I	0.1689
For $\Delta_r/\Delta_0 > 0.43$ $r_{50} = f(\Delta_r/\Delta_0)$	A	0.3804
	B	1.8246
	B	0
For $\Delta_r/\Delta_0 < 0.43$ $r_{50} = f(\Delta_r/\Delta_0)$	A	4.3795E-04
	B	4.9903
	B	3
$l = f(r_{50},a)$	y_0	0.603
	m	0.108
$(S/S_0) = f(a/l)$	$\overline{m}$	0.208

Table 2.2 Empirical relationships to determine modulus

Reference	Material	Prediction Equation	Relationship Statistics	Test Methods[c]	Data validity range
Heukelom and Klomp (1962)	Not indicated	E (MPa) = 9.81 (CBR)	R^2 = 0.89 SE = 59.4	E is calculated from shear wave velocity, three-layer elastic systems , and stiffness measurements[d]	CBR= 2 to 200 E = 34 to 1960 MPa
Powell et al. (1984)	Subgrade materials[a]	E (MPa) = 17.6 (CBR)$^{0.64}$ E[b] (MPa) = 664.67 (PR)$^{-07168}$	Not provided	Laboratory traixial and CBR tests	CBR = 2 to 12 E = no range provided
Pen (1990)	Subgrade[a]	E (MPa) = 1780 (PR)$^{-0.89}$	R^2 = 0.56	E is back-calculated from FWD test using PHONIX program	PR = 12 to 70 mm/blow E = 30 to 250 MPa
		E (MPa) = 4594 (PR)$^{-1.17}$	R^2 = 0.81	E is back-calculated from FWD test using PEACH program	PR = 12 to 70 mm/blow E = 30 to 250 MPa
	Granular base[a]	E (MPa) = 419 (P)$^{-0.85}$	R^2 = 0.73		PR = 1.5 to 10 mm/blow E = 60 to 300 MPa
De Beer (1990)	Granular base and subbase, and subgrade materials[a]	Log (E) (MPa) = 3.05–1.07 log(PR)	R^2 = 0.76 SE = 0.209	E is Back calculated from FWD test using ELSYM program	PR = 0.6 to 25 mm/blow E = 25 to 3,980 MPa
AASHTO (1993)	Fine-grained subgrade[a]	E (MPa) = 10.34 (CBR)	Relationship based on Heukelom and Klomp limiting CBR to < 10		Soaked CBR < 10
Chen et al. (1999)	Lean clay to silt subgrade	E (MPa) = 338 (PR)$^{-0.39}$	R^2 = 0.42 SE = 30.5	E is back-calculated from FWD test using EVERCALC program	PR = 10 to 60 mm/blow E = 62 to 288 MPa
George and Uddin (2000)	Coarse grained sand soil	M_r (MPa) = 235.3 (PR)$^{-0.48}$	R^2 = 0.4 SE = 18.5	M_r determined using laboratory resilient modulus test per AASHTO TP46 on recomapted samples obtained from field	PR = 2.8 to 73 mm/blow M_r = 30 to 160 MPa
	Fine grained sand soil	M_r (MPa) = 532.1 (PR)$^{-0.492}$	R^2 = 0.4 SE = 35.3	M_r determined using laboratory resilient modulus test per AASHTO TP4 on Shelby tube samples obtained from field	PR = 3.8 to 253 mm/blow M_r = 35 to 275 MPa
Konard and Lachance (2001)	Granular base/subbase and granular subgrade	Log (E) (MPa) = –0.884 log(PR) + 2.906	R^2 = 0.92	E is back-calculated from static plate load test using VIEMBACK program	PR = 4 to 11 mm/blow E = 100 to 226 MPa
Nazzal (2003)	Cement treated, lime treated, untreated clay, granular subgrade	Ln (E) (MPa) = 2.35+5.21/ln(PR)	R^2 = 0.91 SE = 0.2	E is back calculated from FWD test using ELMOD 4.0 program provided by Dynatest, Inc.	PR = 5 to 67 mm/blow E = 30 to 240 MPa

(continued)

Reference	Material	Prediction Equation	Relationship Statistics	Test Methods[c]	Data validity range
George (2004)	Medium clay and sand	E (MPa) = 21.83 $(CBR)^{0.478}$	Not provided	M_r determined using laboratory resilient modulus test per AASHTO TP46	Not provided
Chen et al. (2005)	Granular base, chemically stabilized/treated subgrades, and natural subgrade[a]	E (MPa) = 537.76 $(PR)^{-0.6645}$	R^2 = 0.855	E is back calculated from FWD test using MODULUS program	PR = 0.1 to 60 mm/blow
Mohammad et al. (2007)	A-4, A-6, A-7-5, and A-7-6	M_r (MPa) = 151.8/$(PR)^{1.096}$	R^2 = 0.91 SE = 6.1	M_r determined using laboratory resilient modulus test per AASHTO T294	PR = 9 to 65 mm/blow E = 7.6 to 91.4 MPa
Vennapusa et al. (2012)	Well-graded sand, poorly graded sand, and clayey sand	E (MPa) = 1519 $(PR)^{-0.11}$	R^2 = 0.79 SE = 39.5	E is back calculated from FWD test using EVERCALC program	PR = 4 to 18 mm/blow E = 60 to 400 MPa
This Study[e]	Poorly-graded crushed limestone subbase, silty sand subbase, cement treated silty sand subbase, glacial till subgrade, and cement/fly ash treated subgrade	E (MPa) = 73.28-0.15(PR)	R^2 = 0.038 SE = 12.2	E is Back calculated from FWD using the ERIDA program (see text for details)	PR = 23 to 78 mm/blow
		E (MPa) = 323.03$(PR)^{-0.3724}$	R^2 = 0.54 SE = 56.17		PR = 2 to 78 mm/blow
		E (MPa) = 86.11-0.14 (PR)	R^2 = 0.011 SE = 21.97	E is back calculated using AASHTO forward calculation method (see text for details)	PR = 23 to 78 mm/blow
		E (MPa) = 253.94$(PR)^{-0.3044}$	R^2 = 0.38 SE = 56.35		PR = 2 to 78 mm/blow
		E (MPa) = 53.16-0.11(PR)	R^2 = 0.03 SE = 9.78	E is back calculated using Hogg model forward calculation method (see text for details)	PR = 23 to 78 mm/blow
		E (MPa) = 152.35$(PR)^{-0.3024}$	R^2 = 0.50 SE = 26.50		PR = 2 to 78 mm/blow

[a] Type of material is not indicated.
[b] Chen et al. provided the equation to predict E from PR by converting CBR used in Powell et al. equation to PR using CBR = 292/PR1.12.
[c] PR is determined from DCP tests and therefore is repeated in the column, while E and CBR are determined from various test and analysis procedures as indicated.
[d] The type of stiffness method used is not indicated.
[e] The relationships developed using PR of the weakest 75 mm of subgrade are summarized in this paper.
E = elastic modulus, Mr = resilient modulus, SE = standard error, PR = penetration resistance, CBR = California bearing ratio, R2 = coefficient of determination.

Table 2.3 Test section descriptions and testing dates

Project & Section	Year Built	Surface Layer	Base layer	Subgrade Layer	Testing Time
Hamilton Cty. D65	1959-2001	203 mm HMA	152 mm Rolled Stone	Natural Subgrade	08/29/12 04/25/13 10/01/13
Hamilton Cty. 320th St.	2006	178 mm HMA	304 Crushed Limestone Modified Subbase (MSB)	Natural Subgrade	04/25/13 01/10/13
Hamilton Cty. Queens Ave.	2007	178 mm HMA	304 Crushed Limestone MSB	Natural Subgrade	04/25/13 01/10/13
Hamilton Cty. Vail Ave.	2008	101 mm HMA	76 mm Choke Stone + 304 mm Crushed Limestone MSB	Natural Subgrade	08/29/12 04/25/13 10/01/13
Hamilton Cty. D20	2012	127 mm HMA	76 mm Choke Stone + 230 mm Macadam Subbase + 152 mm Road Stone	Natural Subgrade	08/29/12 04/25/13 10/01/13
Boone Expo 1st St.	2013	152 mm HMA	152 mm Crushed Limestone MSB	Compacted Subgrade	04/28/14
Boone Expo 2nd St.	2013	152 mm HMA	152 mm Crushed Limestone MSB + 304 mm Mechanically Stabilized Subgrade	Natural Subgrade	04/28/14
Boone Expo 3rd St.	2013	152 mm HMA	152 mm Crushed Limestone MSB reinforced with 100 or 150 mm Geocells + Non-Woven Geotextile	Natural Subgrade	04/28/14
Boone Expo 4th St.	2013	152 mm WMA	152 mm Crushed Limestone MSB + Woven/Non-Woven Geotextile	Natural Subgrade	04/28/14
Boone Expo 5th St.	2013	152 mm WMA	152 mm Crushed Limestone MSB + Triaxial or Biaxial Geogrid	Natural Subgrade	04/28/14
Boone Expo 7th St.	2013	152 mm HMA	152 mm Crushed Limestone MSB + 152 mm 5% PC Stabilized Reclaimed Subbase	Natural Subgrade	04/28/14
Boone Expo 8th St.	2013	152 mm HMA	152 mm Crushed Limestone MSB	Compacted Subgrade	04/28/14
Boone Expo 9th St.	2013	152 mm. HMA	152 mm Crushed Limestone MSB + 152 mm Reclaimed Subbase	Natural Subgrade	04/28/14
Boone Expo 10th St.	2013	152 mm HMA	152 mm Crushed Limestone MSB	Compacted Subgrade	04/28/14

(continued)

Project & Section	Year Built	Surface Layer	Base layer	Subgrade Layer	Testing Time
Boone Expo 11th St. N	2013	152 mm WMA	152 mm Crushed Limestone MSB	12 in. 11.4% PC stabilized subgrade	04/28/14
Boone Expo 11th St. S	2013	152 mm WMA	152 mm Crushed Limestone MSB	12 in. 22.3% FA stabilized subgrade	04/28/14

Table 2.4 Summary of material gradation properties

Parameter	Hamilton County Test Sites*			Boone Expo Test Sections			
	Choke Stone	**Macadam Subbase**	**Road Stone**	**Crushed Limestone MSB**	**Reclaimed Subbase**	**Mechanically stabilized subgrade**	**Subgrade**
Maximum particle size (mm)	25.4	127.0	25.4	25.4	19.1	19.1	9.5
Gravel Content (%) (>4.75 mm)	59.2	47.5	58.5	65.2	37.2	22.3	5.3
Sand Content (%) (4.75 – 75 μm)	32.1	29.8	20.0	58.1	48.4	46.8	39.7
Silt + Clay content (%) (<75 μm)	8.7	22.7	21.5	7.1	14.4	30.8	55.0
D_{10} (mm)	0.14	0.01	0.05	0.3	0.02	0.001	0.12
D_{30} (mm)	3.1	0.16	1.7	3.6	0.45	0.065	0.01
D_{60} (mm)	9.2	14.7	9.7	10.1	4.0	1.0	—
Coefficient of Uniformity, C_u	65.9	1479.7	199.0	33.7	160	816.3	—
Coefficient of Curvature, C_c	7.2	0.17	6.3	4.3	2.0	3.4	—
Liquid Limit, LL (%)	NP	NP	NP	NP	NP	NP	33
Plasticity Index, PI (%)							15
AASHTO	A-1-a	A-1-b	A-1-a	A-1-a	A-1-a	A-2-4	A-6(5)
USCS Group Symbol	GP	GM	GP-GM	GP-GM	SM	SM	CL

*Gradations presented were obtained from materials used at the D20 test site. Materials with similar descriptions at other sites reportedly have similar gradation properties.

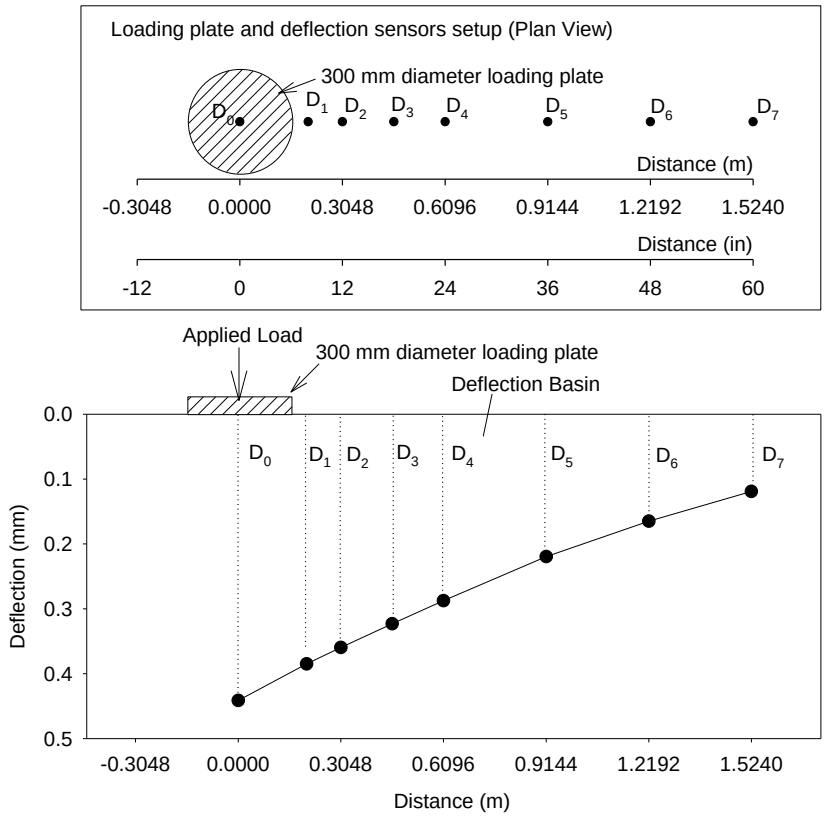

Figure 2.1 FWD testing setup with deflection sensor locations and a typical deflection basin

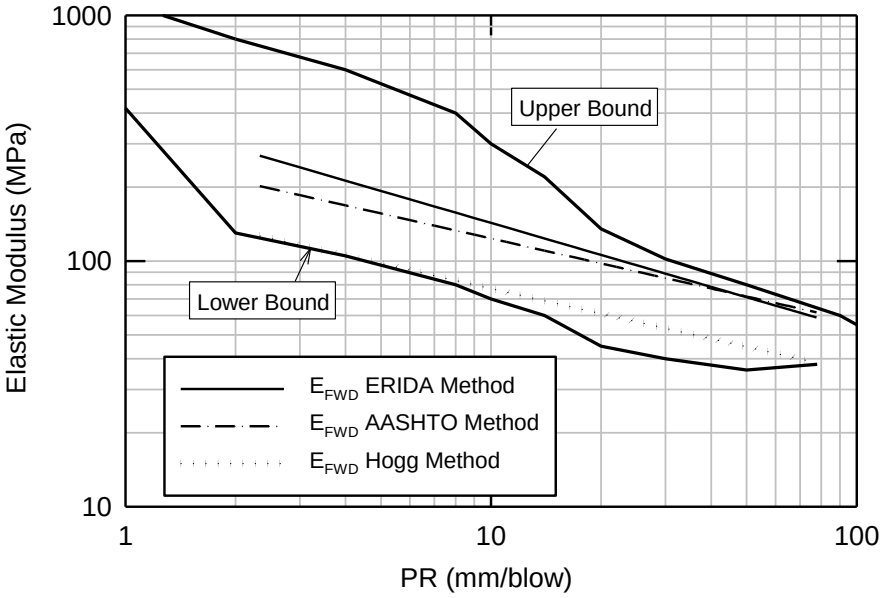

Figure 2.2 Upper and lower bounds of relationships between PR and subgrade/base layer modulus along with relationships observed in this study

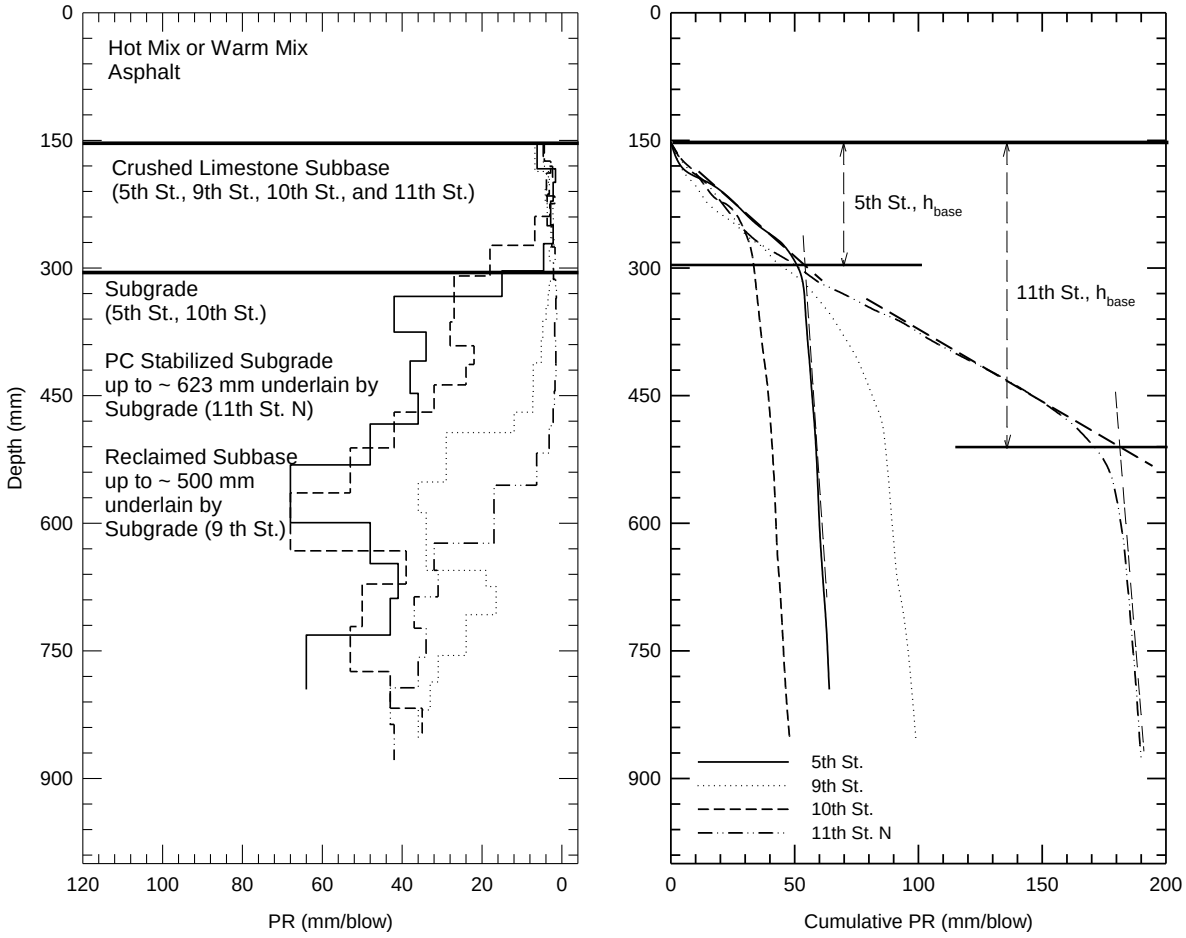

Figure 2.3 Representative PR profiles from DCP test at Boone Expo test sections: (left) showing different foundation support conditions, (right) showing base layer determination

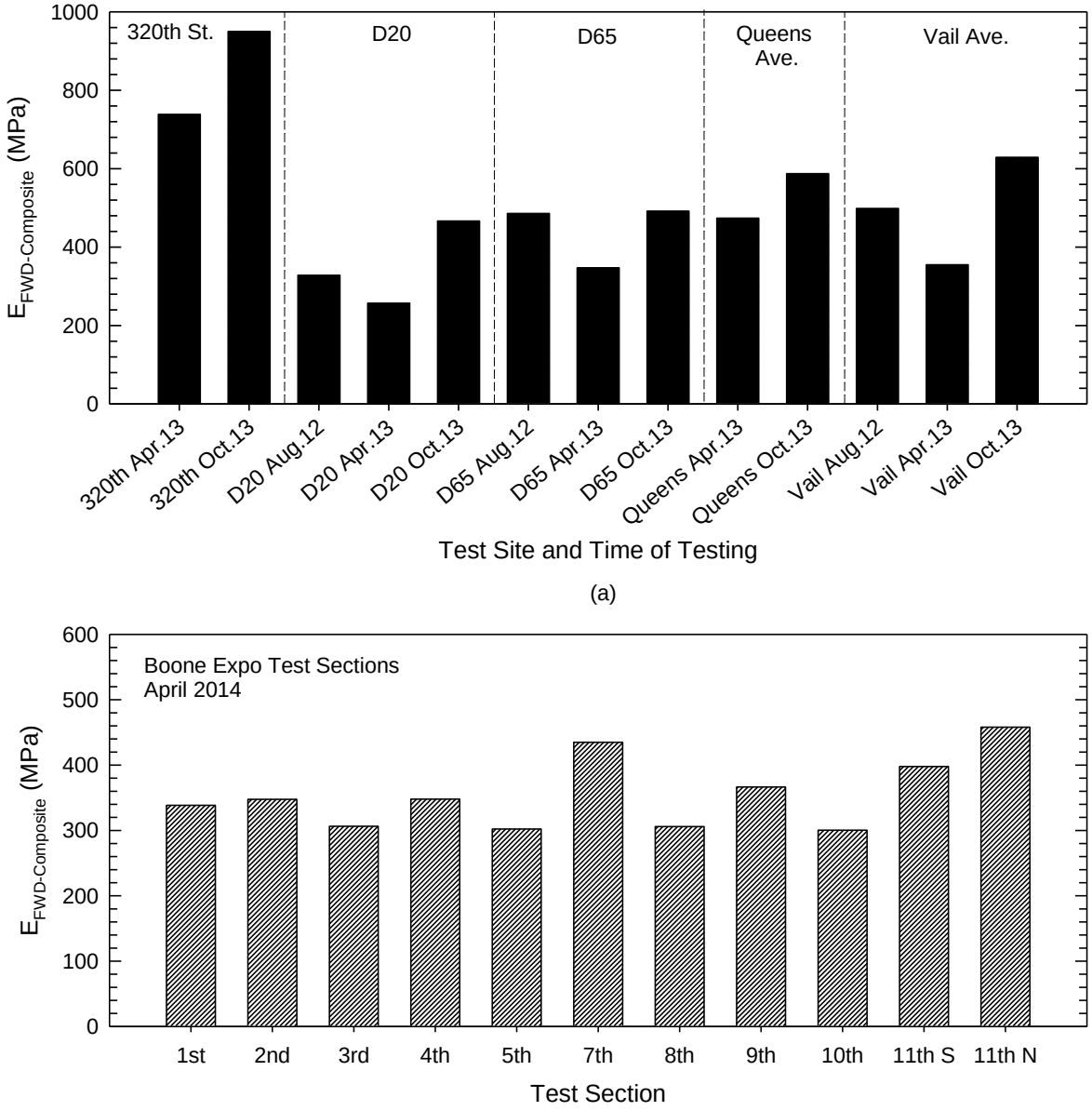

Figure 2.4 Composite FWD modulus measurements on different test sites at different testing times in (a) Hamilton County, and (b) Boone Expo

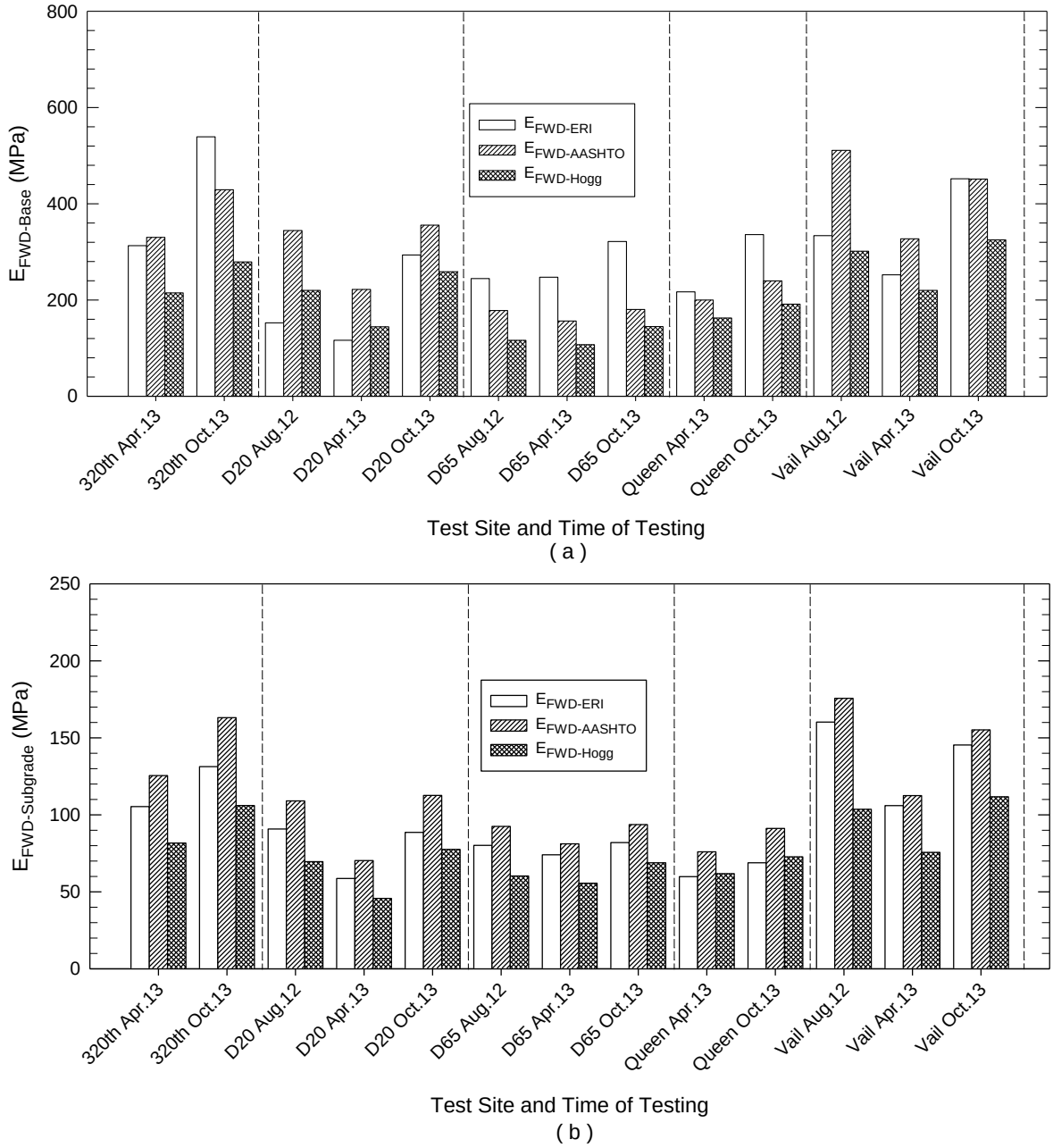

Figure 2.5 Average (a) base and (b) subgrade layer modulus calculated from each method for Hamilton County test sections

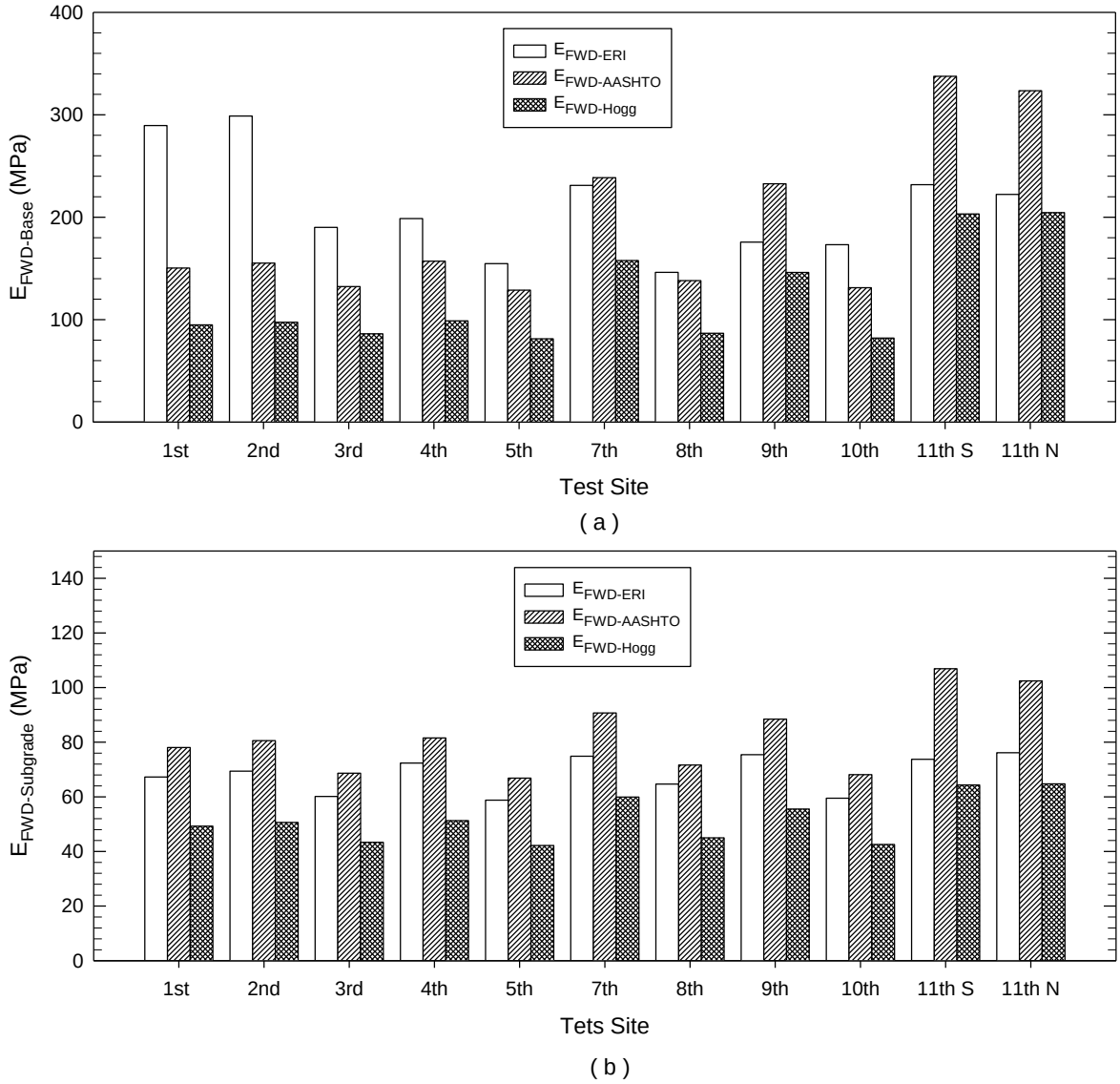

Figure 2.6Average (a) base and (b) subgrade layer modulus calculated from each method for Boone County test section

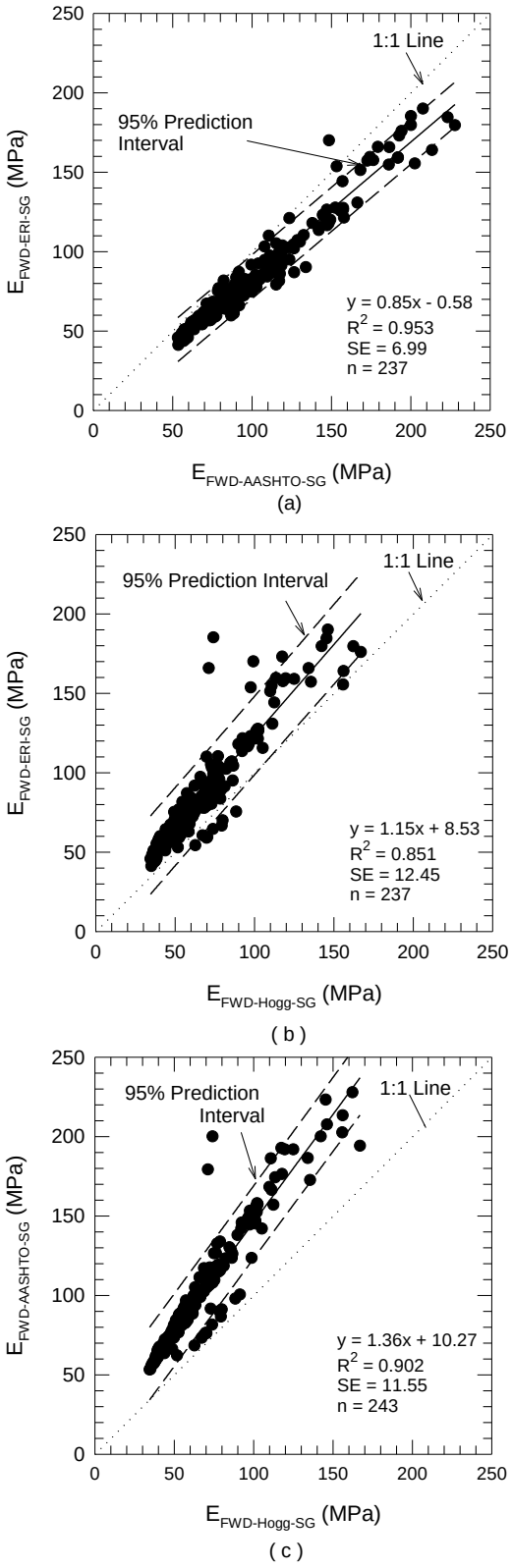

Figure 2.7 Comparison of subgrade layer modulus between each method

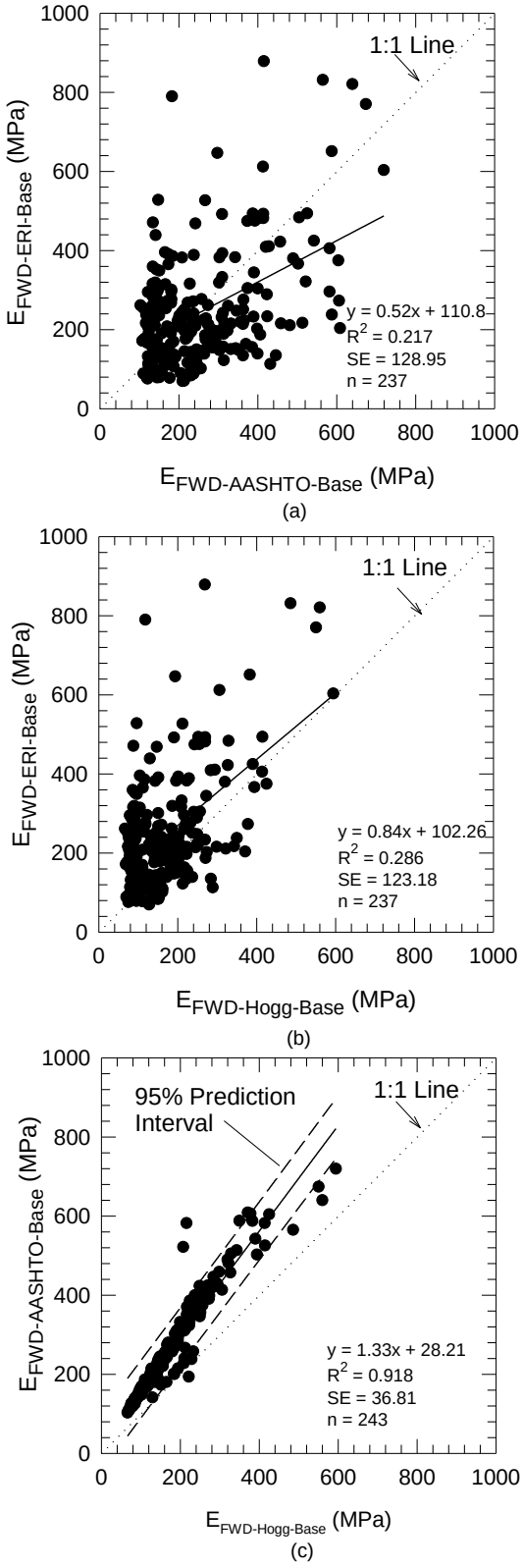

Figure 2.8 Comparison of base layer modulus between each method

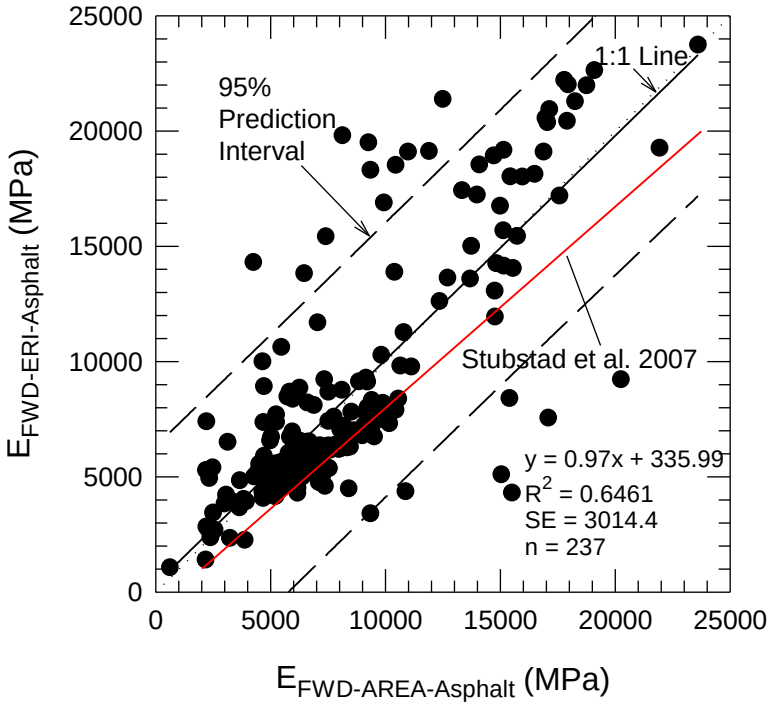

Figure 2.9 Comparison of asphalt surface layer modulus values predicted using backcalculation and forward calculation

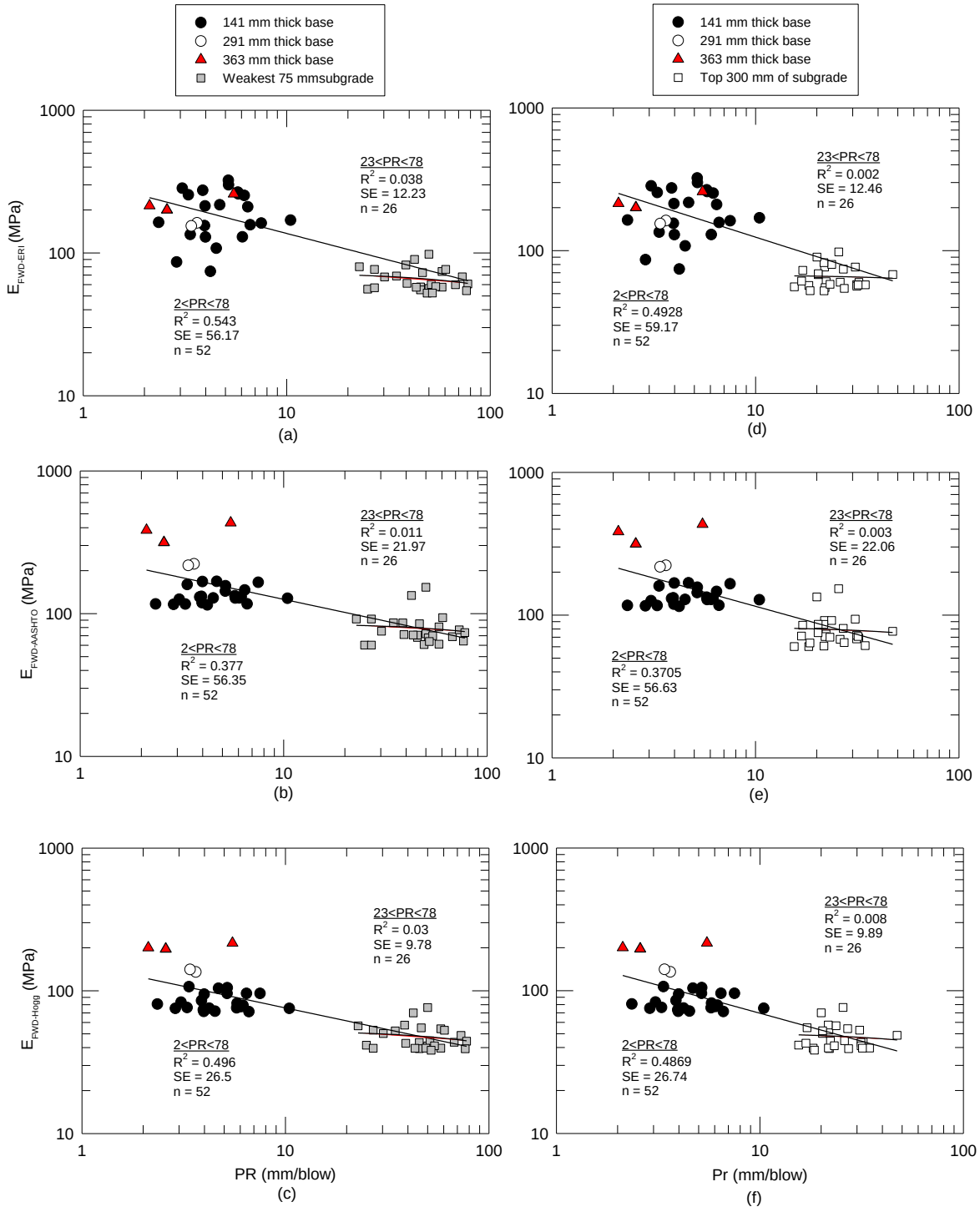

Figure 2.10 Correlations between: (a) $E_{FWD\text{-}ERI}$ and weakest subgrade PR; (b) $E_{FWD\text{-}AASHTO}$ and weakest subgrade PR, (c) $E_{FWD\text{-}Hogg}$ and weakest subgrade PR, (d) $E_{FWD\text{-}ERI}$ and top 300 mm subgrade PR, (e) $E_{FWD\text{-}AASHTO}$ and top 300 mm subgrade PR, (f) $E_{FWD\text{-}Hogg}$ and top 300 mm subgrade PR.

CHAPTER 3. PAVEMENT AND FOUNDATION LAYER ASSESSMENT USING GROUND PENETRATING RADAR

A paper to be submitted to *Nondestructive Testing and Evaluation*

By Jinhui Hu, Pavana K. R. Vennapusa, and David J. White

Abstract

Ground penetrating radar (GPR) surveys are used for pavement assessments in situ to determine layer thicknesses and identify defects beneath pavements. In determining layer thicknesses, the dielectric properties of the materials are typically assumed based on the material type or obtained from field calibrations. This procedure has worked well for pavement surface layers, but variations in material properties and moisture contents in the foundation layers can complicate thickness estimations. In this study, the efficacy of using a ground-coupled GPR system and a hand-held dielectric property measurement device to determine the asphalt and pavement foundation layer thicknesses is assessed. The actual pavement thicknesses were measured from pavement cores and foundation layer thicknesses were measured using dynamic cone penetrometer (DCP). Tests were conducted on various asphalt pavement test sections with different foundation support and drainage conditions, and layer thicknesses. A comparative analysis of core measurements and asphalt layer thicknesses estimated from GPR showed errors < 12%. Base layer thicknesses could not be evaluated using GPR data due to variations in moisture contents. The variations in moisture contents between the test sections are attributed to variations in gradation and permeability properties of the base layer.

Introduction

Ground penetrating radar (GPR) is being increasingly considered in pavement evaluations by highway agencies. GPR survey of existing pavements is a key element of the

rehabilitation design process in the mechanistic empirical pavement design guide (AASHTO 2008) to determine pavement and foundation layer thicknesses for falling weight deflectometer (FWD) analysis. GPR scans are also used to identify defects (e.g., voids, stripping within the asphalt layer, weak bonds between pavement layers) within the pavement layers and beneath the pavement layer; determine depth and alignment of reinforcement in pavements; and determine air void content and density of asphalt layers (Al-Qadi and Lahouar 2005; Al-Qadi et al. 2003; Al-Qadi et al. 2010; Cao et al. 2008; Evans et al. 2008; Lahouar and Al-Qadi 2008). Conducting GPR scans has the advantage of being rapid and less expensive compared to conducting test pits or borings to evaluate existing pavement conditions and it can also capture variations along the pavement alignment.

Dielectric properties of materials being tested is a key parameter in determining layer thickness using GPR. The dielectric properties of layers are either assumed based on published typical values (e.g., Table 3.1), or determined from field calibrations (Al-Qadi and Lahouar 2005), or measured directly using independent test devices (Loizos and Plati 2007) . The field calibration and direct measurement methods have worked fairly well for asphalt materials, although some studies have shown that variations in asphalt moistures can affect the results (Al-Qadi and Lahouar 2005; Al-Qadi et al. 2003; Al-Qadi et al. 2010; Loizos and Plati 2007) . On foundation layer materials, however, the dielectric properties can vary significantly because of moisture and material property variations (Al-Qadi et al. 2003; Grote et al. 2005) demonstrated that GPR data can be used to detect moisture variations within the foundation layers.

This study was undertaken with two objectives. The first objective is to evaluate the efficacy of using a ground-coupled GPR system and a hand-held dielectric property

measurement device called GS3 sensor to determine the asphalt and pavement foundation layer thicknesses. The actual pavement thicknesses were measured from pavement cores and foundation layer thicknesses were measured using dynamic cone penetrometer (DCP). Tests were conducted on various asphalt pavement test sections built at the Central Iowa Expo test site with different foundation support and drainage conditions and layer thicknesses (White et al. 2013). The foundation layers included granular subbase layer underlain by stabilized or unstablized subbase/subgrade layers. A laboratory experimental plan was designed to evaluate dielectric properties of stabilized and unstabilized foundation materials. The second objective is to assess if GPR can be used to detect moisture variations in the unbound layers beneath the pavement. In the following sections of this paper, background information on basic principles of GPR and data analysis, field and laboratory data collection methods followed, results and data analysis, and key findings from this study are provided.

Background

Principles of GPR

GPR uses the principle of transmitting electromagnetic waves to locate changes in subsurface conditions (Fig.3.1). A detailed overview of GPS basic principles is provided by Daniels (2000). In brief, when an electromagnetic wave is transmitted from the antenna, it travels through the material at a velocity depending on the permittivity or dielectric constant of the material, until it hits another object or material with different dielectric properties. When the wave hits a new object or a surface, parts of the wave is “reflected” back to the surface and is captured by the receiver, and parts of the wave continues to travel downward until it is dissipated (or attenuated). The rate of signal attenuation depends on the dielectric

properties and conductivity of the materials. If the materials are highly conductive (e.g., wet clays), the signal is attenuated rapidly (GSSI 2006).

When a series of pulses are sent over a single point, then it is referred to as a scan. The results of a continous scaning of signals are shown as linescan displays or Oscillosope line (O-line). The strength or amplitude of the reflection is determined by the contrast in the dielectric constants of the two materials (GSSI 2006). For example, when a pulse moves from dry sand (with a dielectric constant of about 5) to wet sand (with a dielectric constant of about 30), it will produce a strong reflection. On the other hand, when a pulse moves from dry sand to limestone (with a dielectric constant of about 7) it will not produce a strong reflection.

GPR scanning can be performed using antennas ranging from 16 MHz to 3GHz. The higher the frequency of the antenna, the shallower is the depth of penetration (GSSI 2006). However, the maximum depth of penetration values will be lower when high conductivity materials such as wet clays, ground water table, or underground utilities are encountered.

For pavement applications, 900 MHz to 2GHz antennas are typically used to provide information in the top (0.3 to 1 m). Most highway agencies use horn or air-coupled antenna's where the antenna is located 150 to 500 mm above the surface. These antenna's typically have a frequency range of 1 to 2 GHz. Ground-coupled antennas are in direct contact with the testing surface and typically have a maximum frequency of 1.5 GHz. The air-coupled antennas have advantage over ground-coupled antennas in obtaining data at highway driving speeds. However, as some of the electro-magnetic waves sent by an air-coupled antenna are reflected back from the surface, the depth of penetration is generally lower than a ground-

coupled antenna with similar frequency (Al-Qadi et al. 2003). Ground-coupled antennas limit the survey speed to walking speeds, however, to < 10 km/h.

In ground-coupled antenna scans, the first positive peak produced in the data is referred to as "direct coupling" (GSSI 2006), which occurs in the beginning of the scan and is used to identify the pavement surface position (Fig.3.1). The surface zero position is corrected in the data, by identifying this in the line scans.

Estimating Dielectric Constants of Materials

The material dielectric constants can be estimated based on GPR signals or directly measured using independent test devices. There are two common ways to estimate dielectric constants of materials from GPR signals. One is to use the peak amplitude signals from each layer from a GPR scan in reference to the amplitude signal from a reflective metal surface, and the other is to use the two-way travel time in conjunction with known thickness values. The first method is applicable for air-coupled antennas (Al-Qadi et al. 2003; Cao et al. 2008; Loken 2007), which are not used in this study and is therefore not described here. The two-way travel time method, which is applicable for ground-coupled antennas, was used in this study. According to Loken (2007), the two-way travel time method is not influenced by the errors associated with signal attenuations as in the case of the first method.

The interval of time that it takes for the wave to travel from the transmitter to the receiver is called the two-way travel time. Using the two-way travel times between the different amplitude peaks observed in a wiggle scan, and known layer thickness values, the dielectric constant values can be determined using Eq.1 (Davis and Annan 1989):

$$\varepsilon_r = \left(\frac{ct_i}{2h_i}\right)^2 \quad (1)$$

where,

c = speed of light in air (0.30m/ns),

ε_r = dielectric constant or relative electrical permittivity,

h_i = individual layer thickness, and

t_i = time travel in each individual layer.

There is no widely accepted method in terms of using an independent test device to determine dielectric properties of pavement materials. Loizos and Plati (2007) documented using a hand-held Percometer device in determining dielectric properties of asphalt materials. They found that the location where the dielectric properties were measured (i.e., at the surface or in the middle or a multiple locations on a core), influenced the results. A dielectric probe manufactured by Adek, Ltd. was used by Saarenketo and Scullion (1995). In this study, a GS3 sensor manufactured by Decagon Devices, Inc. was used to measure dielectric properties of asphalt and foundation layer materials. Details of this test device is provided in the following section of this paper.

Moisture Content Determination in Foundation Layers

Moisture content influences the dielectric properties of the materials because the water dielectric constant is much higher (81) than that of air (1) or soil materials (4 to 20). Therefore, high dielectric constants of materials can be attributed to high moistures (Loken 2007). Procedures to estimate gravimetric and volumetric moisture contents have been documented in the literature.

Halabe et al. (1989) used the complex refractive model (CRM) to evaluate relationships between dielectric properties of a material mixture, its volumetric ratios, and dielectric

properties of its components. Using the CBRM, the gravimetric moisture contents of granular base materials can be obtained using Eq.2 (Scullion and Chen 1999):

$$w = (\sqrt{\varepsilon_b} - 1 - \frac{1-n}{\sqrt{\varepsilon_s}-1})/(\sqrt{\varepsilon_b} - 1 - \frac{1-n}{\sqrt{\varepsilon_s}-22.2}) \quad (2)$$

where,

w = moisture content determined as fractional weight of water to total weight;

ε_s = dry aggregate dielectric constant;

ε_b = base layer dielectric constant determined using the two-way travel time method (Eq.1); and

n = porosity = fractional volume of voids (air + water) to total volume.

To determine moisture contents from Eq.2, the porosity of the material has to be either measured or assumed. Maser and Scullion (1992) used Eq.2 by measuring the dry unit weight of granular base material at one location for calibration and the used the same constant value to estimate moisture content at other locations. Comparison between the measured and the predicted moisture contents in their study resulted in root mean squared error of < 2%.

Scullion et al. (1995) reported a procedure that involved developing a laboratory relationship between gravimetric moisture content and dielectric constant, to estimate moisture contents in situ from GPR scans. Results from their study indicated that the relationship between dielectric properties of mixtures increased with increasing moisture content (as expected), and the relationships were unique for each material type.

Grote et al. (2005) used field GPR scans to estimate the dielectric properties of the foundation layers from the two-way travel time method and then estimated material volumetric moisture contents based on laboratory relationships. Site and material specific

relationships between volumetric moisture content and dielectric properties were used in their study for some materials. For materials where those relationships were not available, a third-order polynomial equation developed by Topp et al. (1980) based on tests conducted over a wide range of material types (sandy loam to clay loam to organic soil to glass beads) as shown in Eq.3 was used:

$$\theta_v = 4.3 \times 10^{-6}\varepsilon^3 - 5.5 \times 10^{-4}\varepsilon^2 + 2.92 \times 10^{-2}\varepsilon - 0.053 \quad (3)$$

where,

θ_v = volumetric moisture content; and

ε = material dielectric constant.

Field Test Sections and Experimental Testing Methods

Description of Field Test Sections

The Central Iowa Expo test site located in Boone, Iowa, with various test sections built in 2012-2013 was used for field testing in this study. The foundation layer construction details are summarized in White et al. (2013). The test site consists of 12 roads oriented in north-south direction, labeled from 1st St. to 12th St. a summary of pavement profile in all sections is provided in Table 3.2. Material properties of all foundation layer materials are summarized in Table 3.3.

All streets, expect 6th St., were surfaced with a nominal 152 mm thick hot mix asphalt (HMA) or warm mix asphalt (WMA) layer underlain by a nominal 152 mm thick crushed limestone subbase (CLS) layer. 6th St. is surfaced with concrete pavement and the results are not included in this paper. The HMA and WMA layers varied between the test sections with the type of aggregate used in the mixture, i.e., low or high absorption aggregate (LAA or HAA), as summarized in Table 3.2.

Geocells are used within the CLS layer on 3rd St., and geotextiles and geogrids were used at the CLS and subgrade layer interface on 3rd, 4th, and 5th St. sections. 1st, 3rd, 4th, 5th, 8th, and 10th streets consisted of natural or compacted subgrade layer directly beneath the CLS layer. On 2nd, 7th, 9th, 11th, and 12th St. sections, either a stabilized or unstabilized reclaimed subbase (RSB) or subgrade layer was used between the CLS and subgrade layers, as summarized in Table 3.2. Stabilization of subbase and subgrade layers were performed using mechanical stabilization (i.e., mixing reclaimed subbase and existing subgrade), or by adding Portland cement (PC) or self-cementing Class C fly ash (FA). On 11th St. N, a geocomposite drainage layer (Roadrain T-5 manufactured by Syntec Geosynthetics) was installed directly beneath the asphalt layer.

Metal disks were placed beneath the asphalt surface layer at selected locations to verify the bottom of asphalt layer in GPR scans. An array of temperature sensors (thermistors) were installed on site in the pavement and the foundation layers down to a depth of about 1.4 m below surface for continuous monitoring of temperature variations.

Field and Laboratory Testing Methods

Field and Laboratory GPR Surveys

GPR manufactured by Geophysical Survey Systems, Inc. (GSSI) was used in this study. GPR surveys were conducted on field test sections in September 2013 (fall) and March 2014 (winter). A ground-coupled 900 MHz antenna setup with SIR-20 data acquisition system was used in this study (Fig.3.2 a).

Based on the manufacturer recommendations, the following scan settings were used: (a) range = 15 ns, (b) frequency of scans = 64 Hz, and (c) number of samples per scan = 512.

For GPR scanning conducted in situ, a survey encoder were used to connect the GPR device with a calibrated survey wheel to measure distance. For GPR scanning conducted in laboratory box study (described in detail below), scans were performed in point-mode setting.

Pavement Coring

Iowa Department of Transportation (DOT) performed pavement coring at 58 locations in April 2013, from the various test sections shown in Table 3.2. The core thicknesses were obtained using tape measurement to the nearest 1 mm. Tape measurements were obtained from three locations around the core and was averaged to report the core thickness at each location. The core thicknesses are reported in this paper as h_{core}.

Field DCP Testing

DCP tests were conducted in the foundation layers shortly after the cores were removed. DCP tests were also conducted at various test locations prior to paving. Tests were done at a total of 100 test locations. Testing was done in accordance with ASTM D6951 (ASTM 2003). Penetration resistance (PR) values in units of mm/blow were determined based on the measurements. PR and cumulative blows with depth plots were generated at each test point to determine the base layer thickness. An example plot is shown in Figure 3.4 for reference. The base layer thickness was determined as the depth from the bottom of the asphalt layer to the intersection of the tangents of the upper and lower portions of the cumulative blows with depth curve.

Laboratory Box Testing

Laboratory box testing was conducted in this study to evaluate the GS3 device by comparing ε_{GPR} and ε_{GS3}, on various materials compacted at different target moisture contents. A repeatability study on the two-way travel time method to estimate the ε_{GPR} was

also conducted as part of the box study. The materials included Iowa loess, concrete sand, CLS, and cold mix asphalt (CMA). The index properties of these materials are summarized in Table 3.3.

The materials were compacted in a 762 mm × 304.8 mm × 381 mm wooden box. A metal plate was placed at the bottom of the box as a reflection surface for GPR scans. Tests were conducted on uniform single layer of material with Iowa loess and concrete sand and two- and three-layered structures with loess, CLS, and CMA. The layers were compacted in thin layers (< 30 mm thick) using a hand tamper.

GPR scan and GS3 sensor measurements were simultaneously obtained on the different materials. The two- and three-layered structures were tested at room temperature and after freezing in a temperature chamber for 48 hours (at about -18^{o}C) to assess the influence of frozen versus unfrozen conditions on GPR scans.

Dielectric Constant Determination

Dielectric constant of asphalt and foundation layer materials were directly measured using a GS3 sensor (Fig.3.2b) manufactured by Decagon Devices, Inc., and was also estimated using the two-way travel time method per Eq.1. The dielectric constant measured with the GS3 is reported as ε_{GS3} while the dielectric constant estimated from Eq.1 is reported as ε_{GPR}.

The GS3 device uses capacitance/frequency domain technology to measure soil dielectric constant. The device uses an epoxy body and consists of three stainless steel needles. The device also has a thermistor to measure temperature. According to the Decagon GS3 manual (Decagon 2015), the GS3 device uses an electromagnetic field to measure the dielectric permittivity of the surrounding medium. The sensor supplies a 70 MHz oscillating wave to

the sensor prongs that charges according to the dielectric of the material. According to the manufacturer, the sensor has a measurement influence depth of about 10 cm (Decagon 2015).

The GS3 sensor was used on laboratory compacted specimens and in field on asphalt layers. The laboratory compacted specimens for foundation materials were prepared by compacting materials in accordance with ASTM D698 (ASTM 2013) at various target moisture contents, to assess relationships between gravimetric moisture content (w) and ε_{GS3}. Laboratory testing was conducted on the following materials: loess, subgrade glacial till, CLS, reclaimed subbase (RSB), and Portland cement (PC) and fly ash (FA) treated glacial till subgrade. A nominal 10% PC and 20% FA (by dry weight of soil) was used for treatment. All compacted specimens, except the FA and PC treated subgrade samples, were tested immediately after compaction and after freezing for about 48 hours at about -16 to -17^{o}C. The PC and FA treated subgrade samples were tested at various times after compaction up to about 7 days to assess the influence of curing on ε_{GS3} measurements.

When measuring dielectric constant on laboratory compacted specimens, the GS3 prongs were pushed into the material (Fig.3.3). When material was too hard to push the prongs (i.e., when frozen), three holes that are of same size as the prongs were drilled and then the prongs were inserted into the holes. The same procedure was followed when testing asphalt layers in situ (Fig.3.2b).

Asphalt Layer Thickness Determination in Situ

Asphalt layer thicknesses were directly measured at core locations as explained above. GPR scanning data was used to estimate the asphalt layer thicknesses at the core locations for comparison with the measured thicknesses, using three different procedures.

The first procedure involved the following steps: (1) measure ε_{GS3} from one location in each asphalt mixture type and assume the same at all core locations in the test sections with the same mixture type; (2) convert ε_{GS3} to ε_{GPR} using a relationship developed from the laboratory box study; (3) determine the two-way travel time from the GPR scan at each core location for the asphalt layer; and (4) use the two-way travel time and ε_{GPR} in Eq.1 to estimate the asphalt layer thickness (h_{GPR1}).

The second procedure involved the following steps: (1) determine two way travel times at each core location in sections with same asphalt mixture type; (2) use Eq.1 and h_{core} at each location to calculate ε_{GPR}; (3) average those values for each asphalt mixture; (3) using the two-way travel time at each location and the average ε_{GPR}, estimate the asphalt layer thickness (h_{GPR2}).

The third procedure involved the following steps: (1) determine two-way travel time from the GPR scan at one random core location for each asphalt mixture type; (2) use Eq.1 and the measured h_{core} at the location to determine ε_{GPR} and assume it's the same at all core locations in the test sections with the same mixture type; and (3) determine two-way travel time at the remaining core locations use in Eq.1 to estimate the asphalt layer thickness (h_{GPR3}).

Results and Discussion

Laboratory Box Study Results

GPR scanning test results on two- and three-layered structure in room temperature and after freezing are presented in Figure 3.5. Comparison of results in room temperature and after freezing indicates different two-way travel times. For example, the two-way travel time to the metal sheet was about 8 ns at room temperature, while it was about 6 ns after freezing. In frozen condition, the CLS/loess layer interface is not as clear as in the case of room

temperature. The effect of frozen condition on dielectric properties of the materials is studied with additional testing on laboratory compacted specimens.

Results from the box study comparing ε_{GPR} and ε_{GS3} are shown in Figure 3.6 which yielded a simple linear regression relationship with coefficient of determination (R^2) = 0.95 and standard error (SE) = 1.3.

$$\varepsilon_{GPR} = 1.2146\varepsilon_{GS3} - 0.4614 \quad (4)$$

The relationship suggests that the ε_{GS3} values are slightly lower than ε_{GPR}. The reasons for this difference is attributed to the differences in the measurement influence depths and the measurement errors associated with the two methods. ε_{GPR} represents an average value for the full depth of each layer, while ε_{GS3} only represents the surrounding medium in the depth of penetration.

The repeatability of the two-way travel time method to determine ε_{GPR} was evaluated by obtaining repeated measurements on two-layer and three-layer structures. The results are summarized in Table 3.4, which indicated that the measurement error of ε_{GPR} was < 0.1 for all materials and the percentage error relative to the average value was < 1.5%.

Laboratory Dielectric Constant Measurements on Compacted Specimens

Results showing ε_{GS3} versus gravimetric moisture content (determined on batched materials) immediately after compaction and after freezing are shown in Figure 3.7. The results indicated that ε_{GS3} values increased with increasing gravimetric moisture content for all materials, as expected, and the relationship between ε_{GS3} and moisture content is unique for each material type. In frozen condition, the ε_{GS3} values ranged between 4 and 6 for all materials. This is expected because all free water will be in solid ice phase in frozen

condition and the dielectric constant of pure ice is about 3.4. This is likely the reason why a transition between CLS base and loess in frozen could not be identified in Figure 3.5c.

Figure 3.8 shows ε_{GS3} versus time for chemically stabilized specimens compacted at different moisture contents. As in the case of unstabilized materials, ε_{GS3} increased with increasing moisture content. The ε_{GS3} decreased with curing time up to about 12 hours and then stayed relatively constant. The changes in ε_{GS3} with curing time is attributed to the hydration process where the amount of free water decreases with curing. This was also observed by others in concrete curing process (Pokkukuri 1998). The PC and FA stabilized subgrade showed lower dielectric constant values compared to unstabilized subgrade. For e.g., at about 16% gravimetric moisture content, the unstabilized subgrade showed ε_{GS3} of about 16 and the PC and FA stabilized subgrade showed ε_{GS3} of about 10.

Field Test Results

Results of GPR scans for a portion of a test section from the two testing times are shown in Figure 3.9. Ground temperatures during those times are presented in Figure 3.10, which indicates the foundations layers are in frozen condition in March up to a depth of about 1.3 m below surface. GPR scan obtained during March did not show a transition between subbase and subgrade layers. This was also confirmed during laboratory box study and is attributed to similar dielectric properties in the two layers when frozen.

The measured (h_{core}) and estimated (h_{GPR1}, h_{GPR2}, h_{GPR3}) asphalt layer thicknesses are compared in Figure 3.11. Comparison between the average measured and estimated thickness values for each asphalt mixture type and the average error of the estimates relative to the average measured values are summarized in Table 3.5. The h_{GPR1} values estimated using the

ε_{GS3} values produced values have an average root mean squared error (RMSE) around 17.5 mm compare with the measured values. The h_{GPR3} values estimated using ε_{GPR} estimated from a random core location produced values close to the 1:1 line when compared with the measured values. The RMSE for each mixture type ranged between 4.5 and 14.2 mm, depending on the random location selected in the analysis. When average ε_{GPR} values are used, the estimated h_{GPR2} values reduced the RMSE to 6mm.

GPR scans from September 2013 identified the bottom of the granular base layer (CLS or CLS+RSB layer). On 9th St. test sections where and CLS and RSB layers are present as subbase layers, a clear transition between the two layers could not be identified in the GPR scans, and is therefore analyzed as a single layer. This is attributed to the similar dielectric properties of the two materials as identified in the laboratory testing. The analysis herein is focused only on the CLS and RSB layers.

As the laboratory testing showed strong influence of moisture content on dielectric properties of the subbase layer material, the thickness of the base layers determined from DCP tests and the two-way travel times were used to determine ε_{GPR} of the subbase material. Volumetric moisture contents were determined using ε_{GPR} and Topp et al. (1980) equation (Eq.3) for comparison between the test sections. The purpose of this analysis was to assess variations in the subbase layer moistures between the various test sections. The average ε_{GPR} and volumetric moisture content values determined from DCP test locations are shown in Figure 3.12.

Results indicated that on average, the volumetric moisture contents in the subbase layer varied from about 8% to 30%. The 8th St. test section showed the lowest values. Field

permeability test results documented by White and Vennapusa (2013) on 8th St. South section indicated that the CLS layer on this street showed relatively high saturated hydraulic conductivity and less non-uniformity (Average = 22.7 cm/s and coefficient of variation = 107%), compared to testing performed on 11th St. South section (Average = 1.8 cm/s and coefficient of variation = 172%) and 5th St. South section (Average = 13.2 cm/s and coefficient of variation = 207%). White and Vennapusa (2013) indicated that material on the 8th St. section consisted of more open-graded materials with less segregation and particle degradation compared to 11th St. and 5th St. sections. Field observations showed evidence of segregation and particle degradation due to stiff support conditions on those sections, which resulted in lower permeability values and higher non-uniformity. One limitation of this study is lack of direct volumetric/gravimetric measurements at the test locations at the time of testing to confirm the estimated variations.

Key Findings and Conclusions

Following are some key findings and conclusions from this study:

- Decagon GS3 device was used in this study to measure soil dielectric properties of asphalt and foundation layer materials. The dielectric properties obtained from this device correlated strongly with the dielectric properties back-calculated from GPR with $R^2 = 0.945$ and SE = 1.3.
- This paper provides a new database of dielectric properties of subgrade and base layer materials and chemically stabilized subgrade materials at different moisture contents. Results indicated that the dielectric properties are sensitive to moisture content, as expected. PC and FA stabilized subgrade materials showed lower dielectric values than unstabilized subgrade materials.

- Testing on PC and FA stabilized subgrade materials indicated a reduction in dielectric constant up to about 12 hours and then remained relatively constant after that. This reduction in the first 12 hours is attributed to hydration process in the material.
- GPR surveys conducted during frozen condition did not properly differentiate variations in the foundation layers because of relatively similar dielectric properties of those materials when they are frozen.
- The estimated asphalt thickness values from the field measured ε_{GS3} have an average RMSE about 17.5 mm compare with the measured values. The estimated asphalt thickness values from measured ε_{GPR} at a random core location produced values close to the 1:1 line when compared with the measured values, with RMSE ranging between 4.5 and 14.2mm. When average ε_{GPR} values are used, the average RMSE in the estimated values reduced to 6 mm
- GPR data was used to estimate volumetric moisture content of the granular subbase material. Results indicated that on average, the volumetric moisture contents in the subbase layer varied from about 8 to 30%. The variations are attributed to material segregation and degradation, and variations in aggregate gradations and permeability between the test sections.

References

AASHTO (2008). *Mechanistic-Empirical Pavement Design Guide: A Manual of Practice*, American Association of State Highway Officials and Transportation Officials, Washington, D.C.

Al-Qadi, I., and Lahouar, S. (2005). "Measuring layer thicknesses with GPR–Theory to practice." *Construction and building materials*, 19(10), 763-772.

Al-Qadi, I. L., Lahouar, S., and Loulizi, A. (2003). "GPR: From the State-Of-the-Art to the State-Of-the-Practice."

Al-Qadi, I. L., Lahouar, S., and Loulizi, A. (2003). "Successful application of ground-penetrating radar for quality assurance-quality control of new pavements." *Transportation Research Record*(1861), p. 86-97.

Al-Qadi, I. L., Leng, Z., Lahouar, S., and Baek, J. (2010). "In-place hot-mix asphalt density estimation using ground-penetrating radar." *Transportation Research Record: Journal of the Transportation Research Board*, 2152(1), 19-27.

ASTM (2003). "ASTM D6951 - 03 Standard Test Method for Use of the Dynamic Cone Penetrometer in Shallow Pavement Applications." <http://www.astm.org/DATABASE.CART/HISTORICAL/D6951-03.htm>. (April 18, 2015).

ASTM (2013). "Standard Test Methods for Laboratory Compaction Characteristics of Soil Using Standard Effort (12,400 ft-lbf/ft^3(600 kN-m/m^3))^1." ASTM International, West Conshohocken, PA.

Cao, Y., Guzina, B. B., and Labuz, J. F. (2008). "Pavement Evaluation Using Ground Penetrating Radar." Minnesota Department of Transportation, Maplewood, MN.

Daniels, J. J. (2000). "Ground Penetrating Radar Fundamentals." Prepared as an appendix to Report to the US EPA, Region V (2000), 1-21.

Davis, J. L., and Annan, A. P. (1989). "Ground-penetrating radar for high-resolution mapping of soil and rock stratigraphy." Geophysical Prospecting, 531-551.

Decagon (2015). "GS3 Water Content, EC and Temperature Sensors Operator's Manual." Decagon Devices, Inc., Pullman Washington.

Evans, R., Frost, M., Stonecliffe-Jones, M., and Dixon, N. (2008). "A review of pavement assessment using ground penetrating radar (GPR)." *In 12th International Conference on Ground Penetrating Radar*Birmingham, UK.

Grote, K., Hubbard, S., Harvey, J., and Rubin, Y. (2005). "Evaluation of infiltration in layered pavements using surface GPR reflection techniques " *Journal of Applied Geophysics*, 57(2), 129-153.

GSSI (2006). "GSSI Handbook For RADAR Inspection of Concrete." Geophysical Survey Systems, Inc, Salem, New Hampshire.

Halabe, U. B., Maser, K., and Kausel, E. (1989). "Condition Assessment of Reinforced Concrete Using EM Waves." Massachusetts Institute of Technology, Cambridge, Mass.

Hubbard, S. S., Peterson, J. E., Majer, E. L., Zawislanki, P. T., Williams, K. H., Roberts, J., and Wobber, F. (1997). "Estimation of permeable pathways and water content using tomographic radar data." *The leading Edge*, 16(11), 1623-1630.

Lahouar, S., and Al-Qadi, I. L. (2008). "Automatic Detection of Multiple Pavement Layers From GPR Data." *NDT & E International*, 41(2), 69-81.

Loizos, A., and Plati, C. (2007). "Accuracy of pavement thicknesses estimation using different ground penetrating radar analysis approaches." *NDT & E International*, 40(2), 147-157.

Loken, M. C. (2007). "Use of Ground Penetrating Radar to evaluate Minnesota Roads." Minnesota Department of Transportation, Research Services Section, Maplewood, MN.

Lucius, J. E., Olhoeft, G. R., Hill, P. L., and Duke, S. K. (1989). "Properties and hazards of 108 selected substances." U.S. Geological Survey.

Martinez, A., and Alan P. Byrnes (2001). "Modeling dielectric-constant values of geologic materials: An aid to ground-penetrating radar data collection and interpretation." Kansas Geological Survey, University of Kansas.

Maser, K., and Scullion, T. (1992). "Influence of Asphalt Layering and Surface Treatments on AsphaltBase Layer Thickness Computations Using Radar." Report No. TX-92-1923-1, Texas Transportation Institute.

Olhoeft, G. R. (1989). "Electrical properties of rocks; in, Physical Properties of Rocks and Minerals." Hemisphere Publishing Corporation, New York, 257–329.

Pokkukuri, K. S. (1998). "Effect of Admixtures, Chlorides, and Moisture on Dielectric Properties of Portland cement Concrete in the Low Microwave Frequency Range " M.S., Virginia Polytechnic Institute and State University.

Saarenketo, T., and Scullion, T. (1995). "Using electrical properties to classify the strength properties of base course aggregates." Texas Transportation Institute, College Station, Texas.

Scullion, T., Chen, Y., and Lau, C. L. (1995). "COLOMAP-user's Manual with Case Studies." Texas Transportation Institute Report, 1341-1, College Station, Texas.

Topp, G. C., Dadvis, J. L., and Annan, A. P. (1980). "Electromagnetic determination of soil water content: measurements in coaxial transmission lines." *water Resour. Res.*, 16(3), 574-582.

White, D., Vennapusa, P., Becker, P., and Rodrigez, J. (2013). "Central Iowa Expo Pavement Test Sections: Phase I – Foundation Construction." Center for Earthworks Engineering Research Iowa State University, InTrans Project 12-433, Ames, IA

White, D. J., Becker, P., Vennapusa, P. K., Dunn, M. J., and White, C. I. (2013). "Assessing Soil Stiffness of Stabilized Pavement Foundations." *Transportation Research Record: Journal of the Transportation Research Board*, 2335(1), 99-109.

Table 3.1 Typical dielectric properties of pavement and foundation layer materials

Material	Dielectric constant	Reference
Air	1	Lucius et al. (1989)
Asphalt	3-6	Cao et al. (2008)
Concrete	6-11	Cao et al. (2008)
Ice	3.4	Olhoeft (1989)
Dry Sand	3-5	Martinez A. and Alan P. (2001)
Wet Sand	20-30	Martinez A. and Alan P. (2001)
Limestone	4-8	Hubbard et al. (1997)
Limestone (0 to 12% moisture content)	4-22	Saarenketo and Scullion (1995)
Dolomite (0 to 12% moisture content)	4-17	Saarenketo and Scullion (1995)
Sandstone (0 to 12% moisture content)	4-17	Saarenketo and Scullion (1995)
Caliche Gravel (0 to 10% moisture content)	5-22	Saarenketo and Scullion (1995)
Iron Ore Gravel (0 to 16% moisture content)	2-16	Saarenketo and Scullion (1995)
Silts	5-30	Hubbard et al. (1997)
Clay (dry to moist)	5-40	Hubbard et al. (1997)
Water	81	Lucius et al. (1989)
Glacial till (10%-23% moisture content)	9-20	This Study
Iowa loess (10%-23% moisture content)	6-17	
Crushed limestone (5%-12% moisture content)	5-16	
Reclaimed subbase (5%-13% moisture content)	6-15	
10% Portland cement treated glacial till after curing (7%-16% moisture content)	6-10	
20% fly ash treated glacial till after curing (7%-16% moisture content)	5-11	

Table 3.2 Summary of field tests sections

Section	Surface Layer	Base layer	Intermediate Layer	Subgrade Layer
1st St. N and S	152 mm HMA with LAA[a]	152 mm CLS	—	Compacted Subgrade
2nd St. N and S	152 mm HMA with LAA[a]	152 mm CLS	304 mm Mechanically Stabilized Subgrade	Natural Subgrade
3rd St. N	152 mm HMA with LAA[a]	152 mm CLS reinforced with 100 mm Geocells	Non-Woven Geotextile	Natural Subgrade
3rd St. S	152 mm WMA with LAA[a]	152 mm CLS reinforced with 150 mm Geocells	Non-Woven Geotextile	
4th St. N	152 mm WMA with LAA[a]	152 mm CLS	Non-Woven Geotextile	Natural Subgrade
4th St. S			Woven Geotextile	
5th St. N	152 mm WMA with LAA[a]	152 mm CLS	Triaxial geogrid	Natural Subgrade
5th St. S			Biaxial geogrid	
7th St. N and S	51 mm HMA with HAA[b] + 102 mm HMA with LAA[a]	152 mm CLS	152 mm 5% PC Stabilized Reclaimed Subbase	Natural Subgrade
8th St.	51 mm HMA with HAA[b] + 102 mm HMA with LAA[a]	152 mm CLS	—	Compacted Subgrade
9th St.	51 mm HMA with HAA[b] + 102 mm HMA with LAA[a]	152 mm CLS	152 mm Reclaimed Subbase	Natural Subgrade
10th St. N	51 mm WMA with HAA[b] + 102 mm HMA with LAA	152 mm CLS	—	Compacted Subgrade
10th St. S			—	Natural subgrade
11th St. N	51 mm WMA with HAA[b] + 102 mm WMA with LAA	152 mm CLS	12 in. 11.4% PC stabilized subgrade	Natural subgrade
11th St. S			12 in. 22.3% FA stabilized subgrade	

[a]Low absorption aggregate.
[b]High absorption aggregate.

Table 3.3 Summary of material index properties

Parameter	CLS	RSB	Concrete Sand	Iowa Loess	Glacial Till Subgrade
Gravel Content (%) (> 4.75 mm)	65.2	37.2	2.2	0.0	5.3
Sand Content (%) (4.75 – 75 μm)	58.1	48.4	96.2	2.9	39.7
Silt + Clay content (%) (<75μm)	7.1	14.4	1.6	103.7	55.0
D_{10} (mm)	0.3	0.02	0.28	–	0.12
D_{30} (mm)	3.6	0.45	0.57	0.013	0.01
D_{60} (mm)	10.1	4.0	1.2	0.028	–
Coefficient of Uniformity, C_u	33.7	160	4.22	–	–
Coefficient of Curvature, C_c	4.3	2.0	0.95	–	–
Liquid Limit, LL (%)	NP	NP	NP	29	33
Plasticity Index, PI (%)				23	15
AASHTO Classification	A-1-a	A-1-a	A-1-b	A-4	A-6(5)
USCS Group Symbol	GP-GM	SM	SP	ML	CL

Table 3.4 Summary of repeatability in determine dielectric properties from two way travel time

	Two layer system		Three layer system in room temperature			Three layer system in frozen condition	
Statistical parameters	**CLS**	**Loess**	**CMA**	**CLA**	**Loess**	**CMA**	**CLS+Loess**
Number of measurements	28	28	24	24	24	31	31
Average ε_{GPR}	11.02	12.74	6.55	6.12	15.57	4.87	4.73
Standard deviation or measurement error of ε_{GPR}	0.08	0.09	0.09	0.04	0.08	0.07	0.02
Percentage error*	0.7%	0.7%	1.4%	0.7%	0.5%	1.4%	0.4%

*calculated as 100 x standard deviation of ε_{GPR} / average ε_{GPR}

Table 3.5 Comparison between average asphalt thicknesses measured from core and different predicted from GPR scans and percentage errors in predictions

Street	Asphalt layer description	No. of Measurements	Average h_{core} (mm)	h_{GPR1} (mm)		h_{GPR2} (mm)		h_{GPR3} (mm)	
				Average	RMSE[e]	Average	RMSE[e]	Range	RMSE[e]
1st / 2nd	50 mm HMA[a] surface with LAA[c] 102 mm HMA[a] base with LAA[c]	16	163.3	178.8	16.9	163.2	5.8	156.3-175.6	6.3-13.9
3rd S. / 4th	50 mm WMA[b] surface with LAA[c] 102 mm WMA[b] base with LAA[c]	10	165.5	183.5	18.7	165.5	4.5	160.9-175.6	4.5-8.5
7th / 8th	50 mm HMA[a] surface with HAA[d] 102 mm HMA[a] base with LAA[c]	16	165.4	182.2	18.3	165.1	8.8	155.7-184.0	8.8-14.2
9th S. / 10th	50 mm WMA[b] surface with HAA[d] 102 mm HMA[a] base with LAA[c]	11	160.1	173.9	15.2	159.8	6.1	151.0-169.9	7.7-11.6
11th	50 mm WMA[b] surface with HAA[d] 102 mm WMA[b] base with LAA[c]	5	163.8	181.6	18.7	163.7	5.0	157.2-172.7	5.6-10.4

[a]Hot mix asphalt.
[b]Warm mix asphalt.
[c]Low absorbed aggregate.
[d]High absorbed aggregate.
[e]Root mean squared error estimated to the measured values.

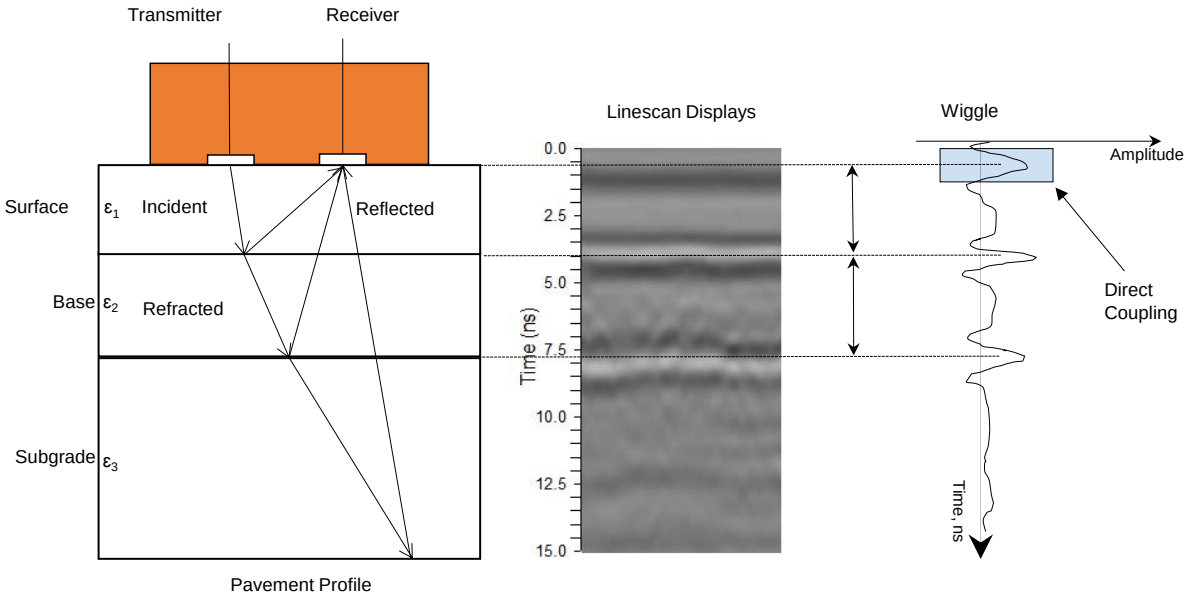

Figure 3.1 Ground penetrating radar principles

(a)

(b)

Figure 3.2 In situ (a) GSSI GPR with a 900 MHz antenna and SIR-20 data acquisition system and (b) Decagon GS3 dielectric sensor

Figure 3.3 Laboratory dielectric constant measurement on a compacted crushed limestone sample

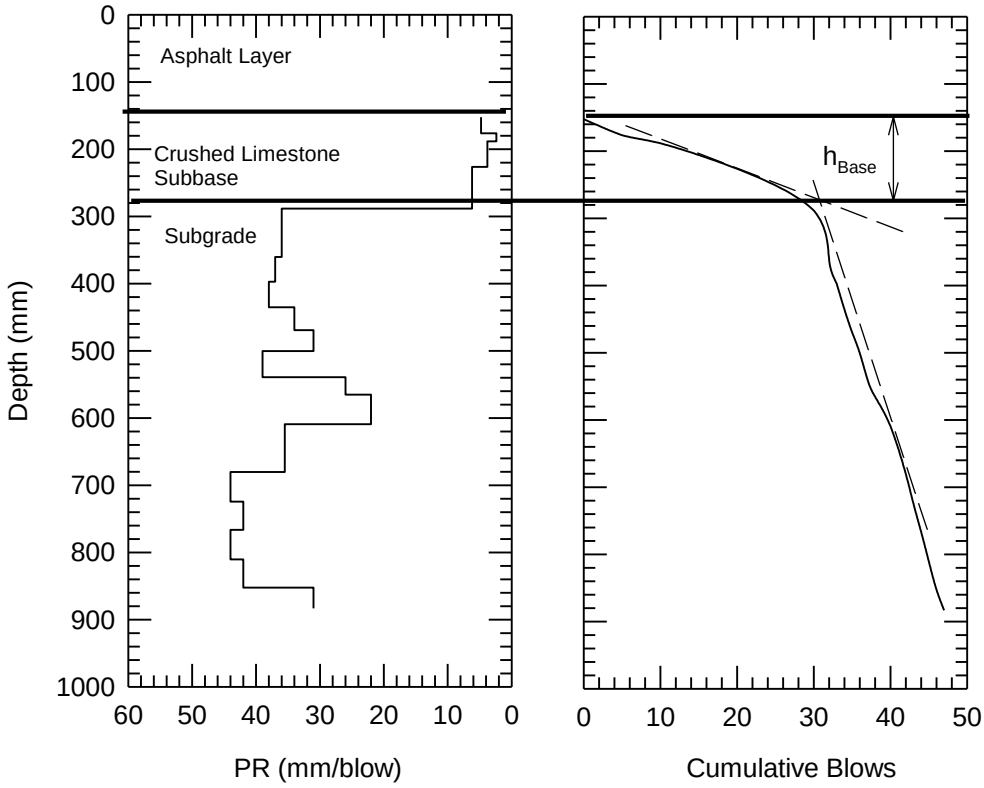

Figure 3.4 Example penetration resistance and cumulative blows with depth profiles used for base layer thickness determination

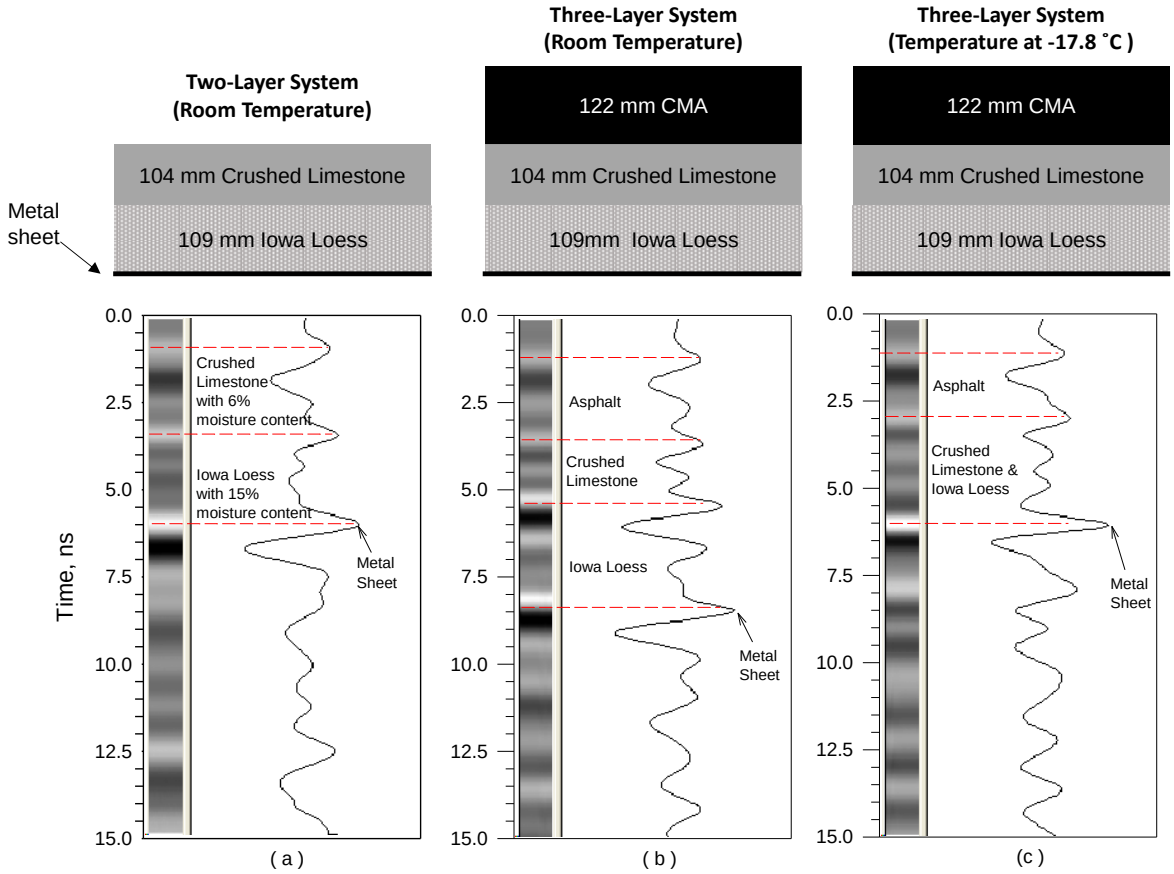

Figure 3.5 Results of laboratory box study with (a) two layered profile at room temperature, (b) three layered profile at room temperature, and (c) three layered profile frozen at -17.8ºC for 48 hours

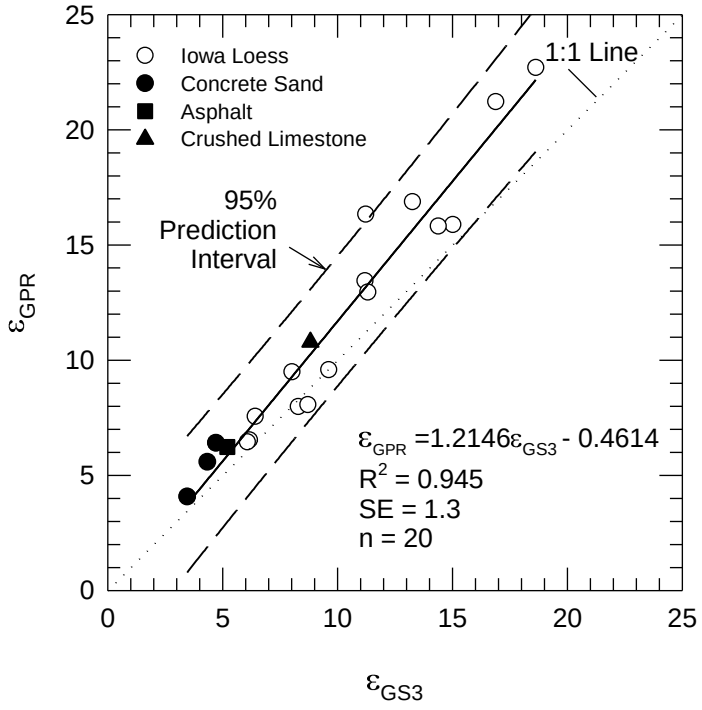

Figure 3.6 Dielectric constant values determined from GPR (ε_{GPR}) and GS3 sensor (ε_{GS3})

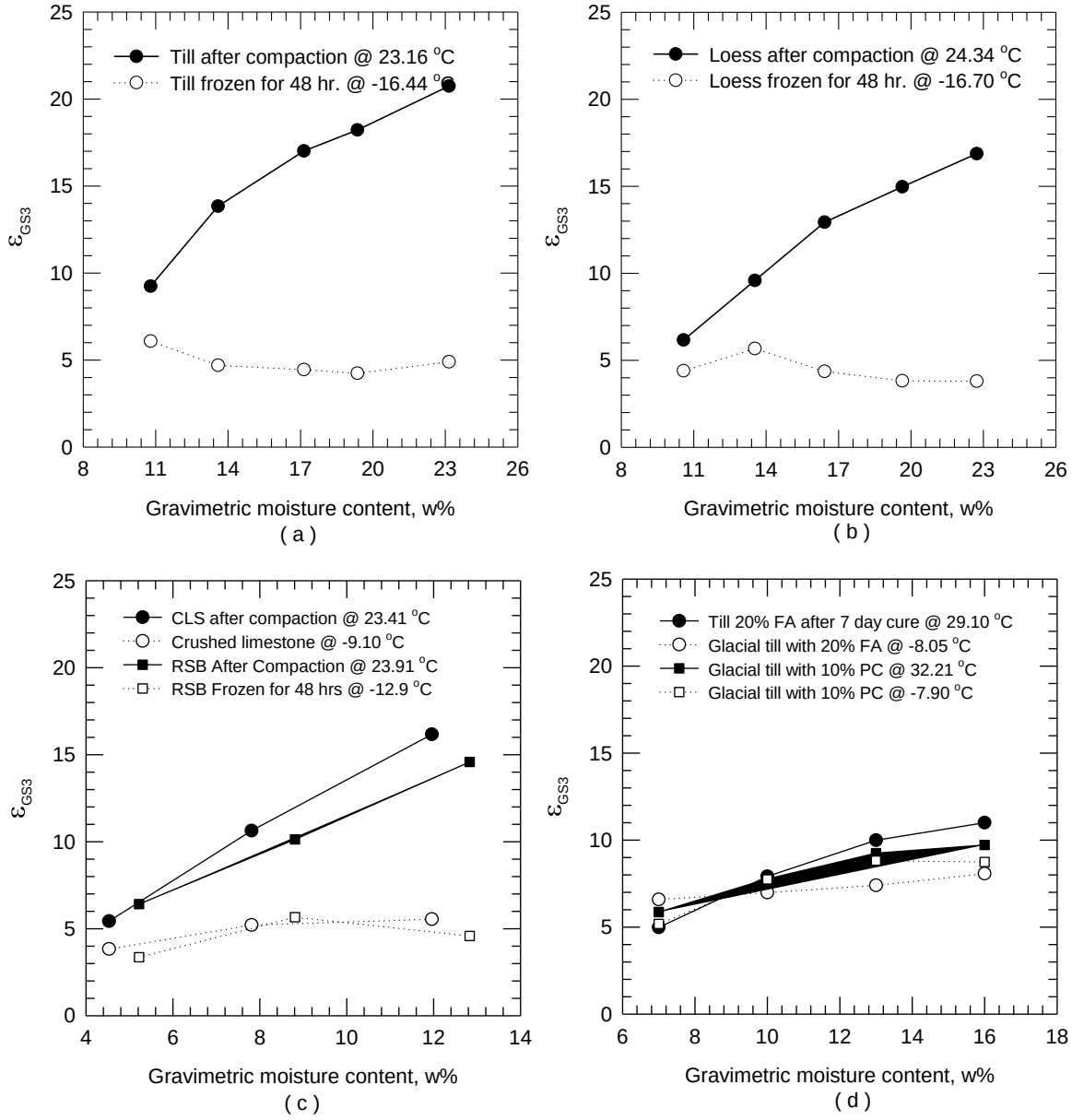

Figure 3.7 ε_{GS3} versus gravimetric moisture content on: (a) glacial till subgrade, (b) Iowa loess, (c) CLS and RSB, and (d) glacial till treated with PC and FA

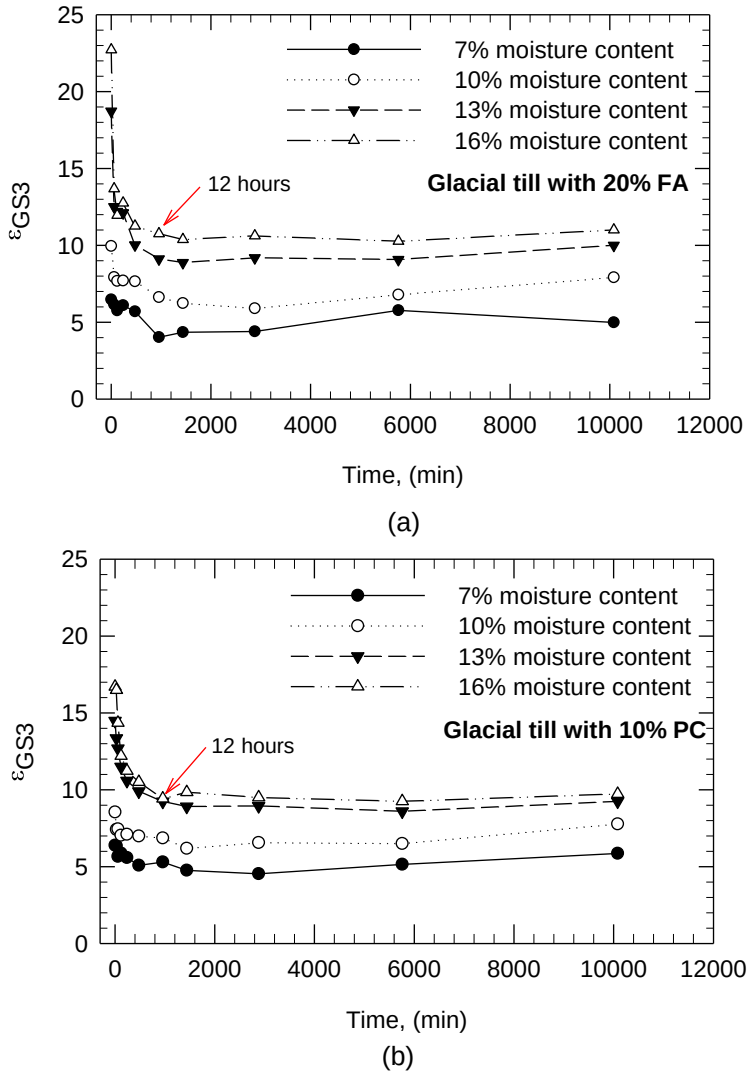

Figure 3.8 Laboratory measured ε_{GS3} on chemically stabilized glacial till subgrade at different moisture contents after different curing times: (a) stabilized with 20% FA, (b) stabilized with 10% PC

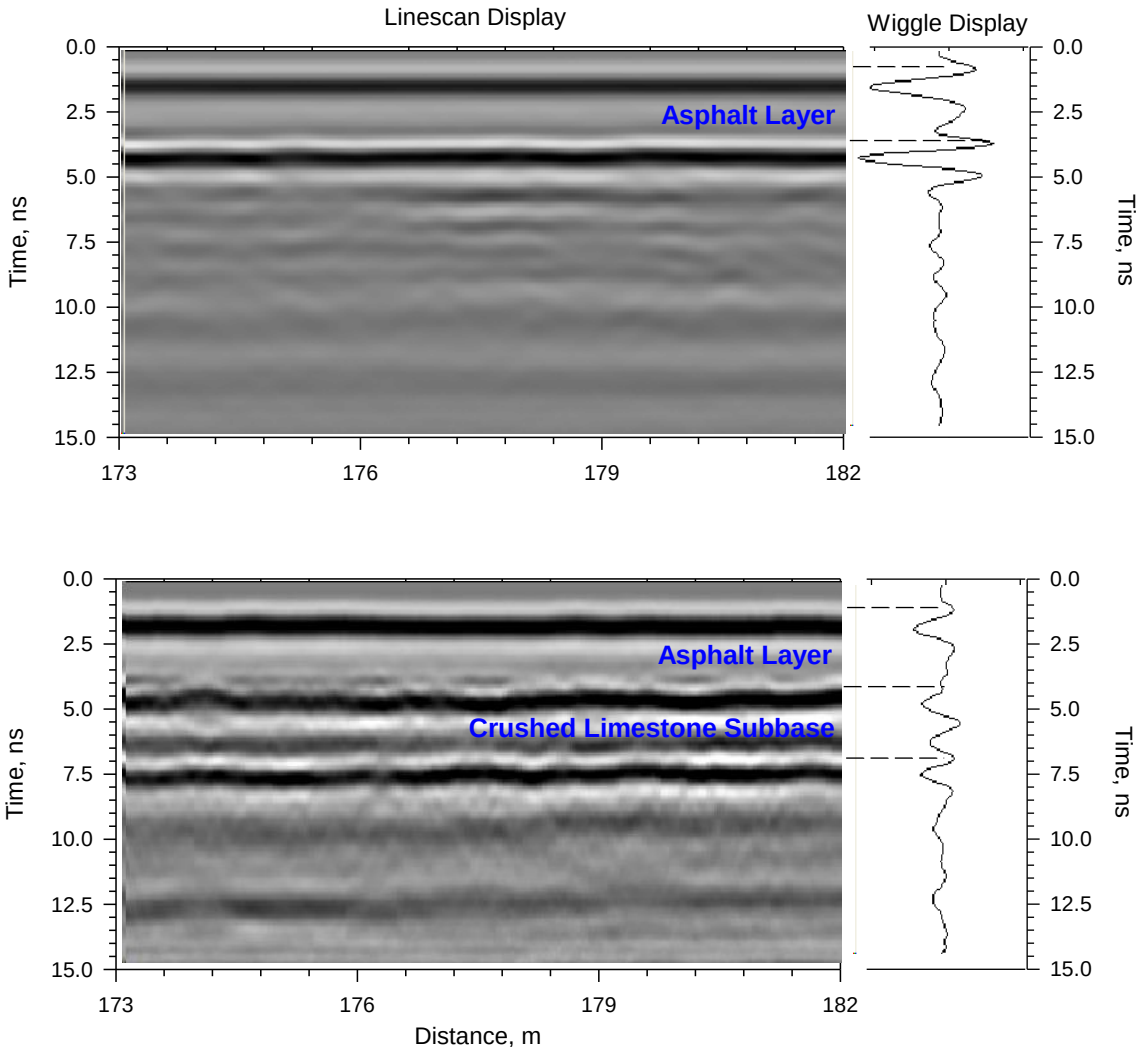

Figure 3.9 In situ GPR scan on 10th street south section, (a) tested on 03/12/14, (b) tested on 09/16/14

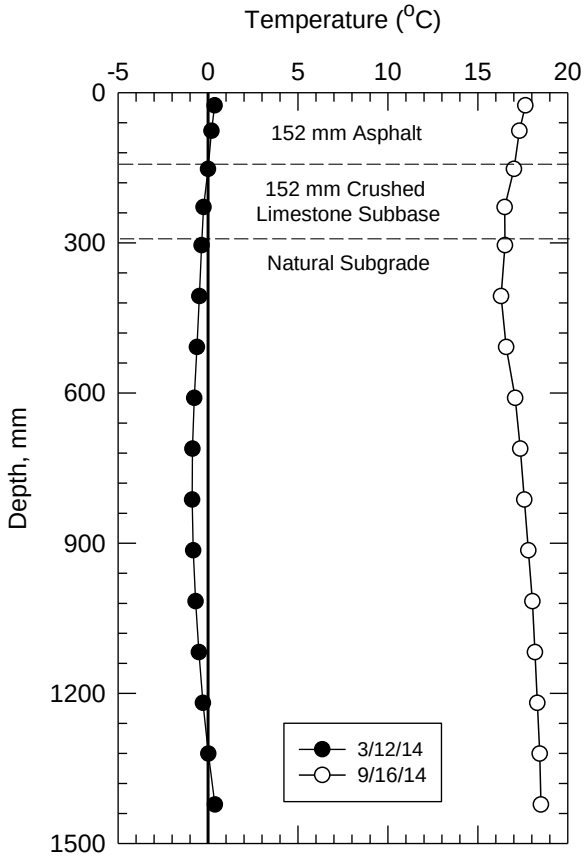

Figure 3.10 In situ ground temperatures during the two testing times

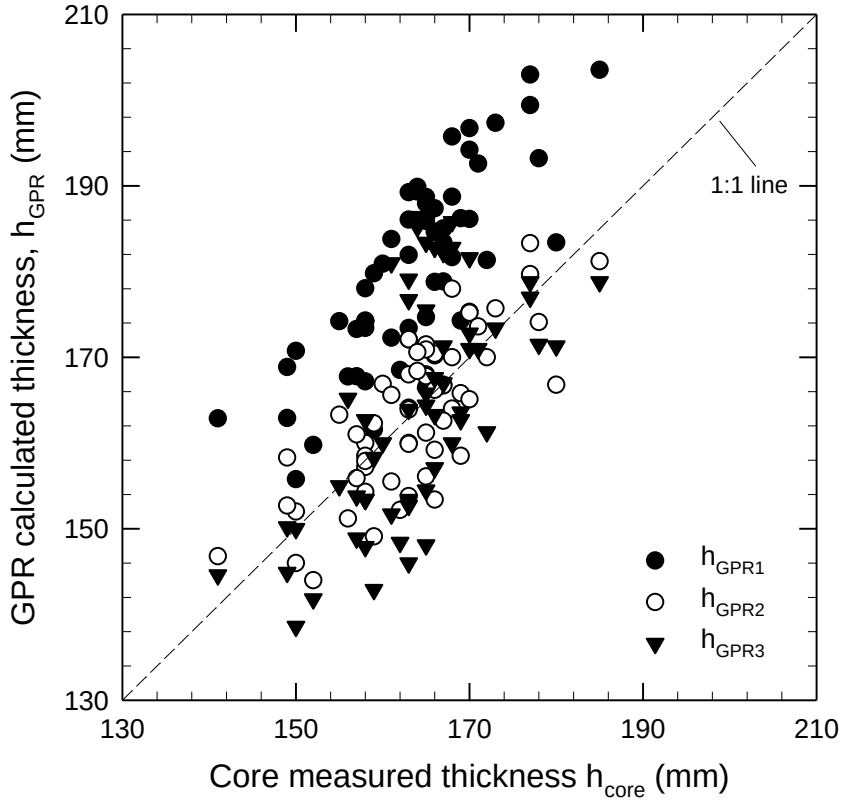

Figure 3.11 Comparison of GPR estimated h_{GPR} and core measured asphalt layer thickness h_{core}

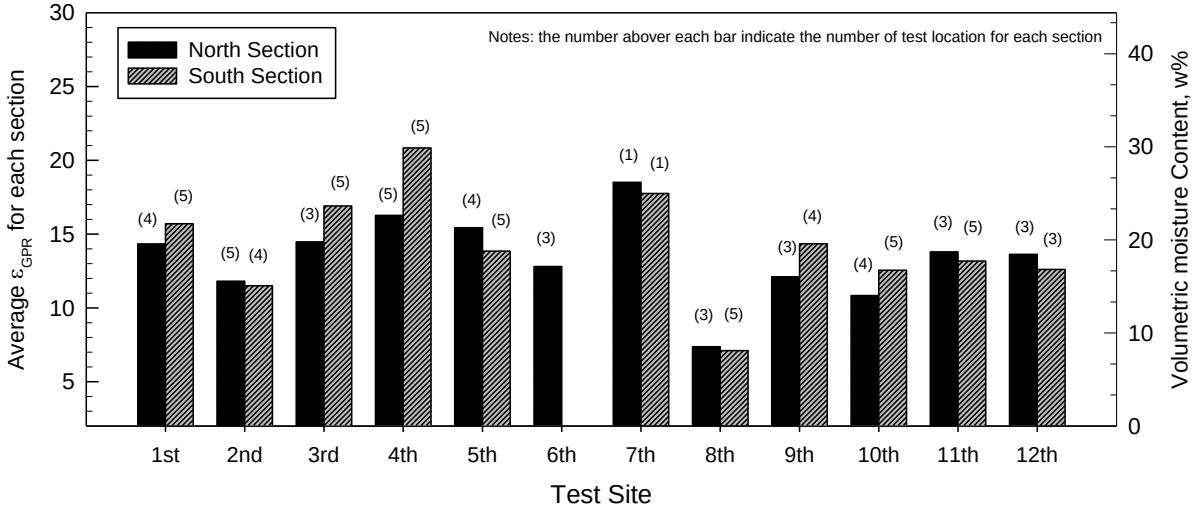

Figure 3.12 Estimated average in situ base layer ε_{GPR} and gravimetric moisture contents for each street based on DCP test measurements at 1 to 6 location

CHAPTER 4. CONCLUSIONS AND RECOMMENDATIONS

This study presents the evaluation of two nondestructive devices FWD and GPR in pavement assessment. Variation test sites were selected in this experiment, each test site is vary with pavement thickness and support conditions. Limited coring and DCP tests were conducted for verification purposes. The FWD data interpretation paper intended to demonstrate the uncertainty of using different analysis methods, and the risk of using DCP test to estimate pavement layer modulus. The GPR data interpretation paper intended to evaluate the accuracy of using GPR to determine asphalt layer thickness and the viability of using GPR to estimate foundation moisture content. The following sections provide the general conclusions and recommendations for future research and practice.

Conclusions

The following are the key findings from this research:

- The AASHTO and Hogg forward calculation methods and ERIDA backcalculation program produced subgrade moduli values that are strongly correlated with R^2 between 0.85 and 0.95 and SE < 13 MPa. However, the AASHTO and ERIDA methods produced subgrade moduli values that are 1.28 and 1.51 times higher than the Hogg method.
- Base layer modulus calculations showed significant variations between the Dorman and Metcalf forward calculation and the ERIDA back calculation method. Regression relationships between forward and backcalculated moduli values yielded low R^2 values (< 0.3) and high SE values (> 120 MPa).
- Regression analysis between the backcalculated and forward calculated asphalt layer moduli values yielded a linear relationship that is close to the 1:1 line with $R^2 = 0.65$.

However, there was significant scatter in the data with a standard error of about 3,000 MPa.

- New relationships between PR and moduli values calculated from three forward and back calculation methods for a PR range of 2 and 78 mm/blow are presented in this paper. The relationships indicated that for if data over PR = 2 to 78 mm are considered, the standard error of the estimate ranged from 24 to 60 MPa, depending on the modulus calculation method. The standard error of the estimate decreased to < 20 MPa, when data from PR = 23 to 78 (i.e., only subgrade) are considered.
- The estimated asphalt thickness values from the field measured ε_{GS3} have an average RMSE about 17.5 mm compare with the measured values. The estimated asphalt thickness values from measured ε_{GPR} at a random core location produced values close to the 1:1 line when compared with the measured values, with RMSE ranging between 4.5 and 14.2mm. When average ε_{GPR} values are used, the average RMSE in the estimated values reduced to 6 mm
- This paper provides a new database of dielectric properties of subgrade and base layer materials and chemically stabilized subgrade materials at different moisture contents. Results indicated that the dielectric properties are sensitive to moisture content, as expected. PC and FA stabilized subgrade materials showed lower dielectric values than unstabilized subgrade materials.
- Testing on PC and FA stabilized subgrade materials indicated a reduction in dielectric constant up to about 12 hours and then remained relatively constant after that. This reduction in the first 12 hours is attributed to hydration process in the material.

- GPR surveys conducted during frozen condition did not properly differentiate variations in the foundation layers because of relatively similar dielectric properties of those materials when they are frozen.
- GPR data was used to estimate volumetric moisture content of the granular subbase material. Results indicated that on average, the volumetric moisture contents in the subbase layer varied from about 8 to 30%. The variations are attributed to material segregation and degradation, and variations in aggregate gradations and permeability between the test sections.

Recommendations for Future Research and Practice

The following are recommendations for future research and practice:

- A long-term goal would be to develop more precise methods for interpreting data from nondestructive test methods.
- Because many agencies use empirical relationships and typical parameters for pavement design and for making decisions about pavement rehabilitation, it is important to understand the uncertainties involved in interpreting data obtained from nondestructive methods such as FWD, DCP, and GPR.
- GPR has the potential to evaluate the efficiency of base layer drainage conditions and merits future study.
- GPR scanning to evaluate pavement layer thickness is not recommended when ground is frozen because the water phase change from liquid to solid results in low contrast between dielectric properties of different materials.